



**HAL**  
open science

**Bony pseudoteeth of extinct pelagic birds (Aves, Odontopterygiformes) formed through a response of bone cells to tooth-specific epithelial signals under unique conditions**

Antoine Louchart, Vivian De Buffrénil, Estelle Bourdon, Maitena Dumont, Laurent Viriot, Jean-Yves Sire

► **To cite this version:**

Antoine Louchart, Vivian De Buffrénil, Estelle Bourdon, Maitena Dumont, Laurent Viriot, et al.. Bony pseudoteeth of extinct pelagic birds (Aves, Odontopterygiformes) formed through a response of bone cells to tooth-specific epithelial signals under unique conditions. *Scientific Reports*, 2018, 8 (1), 10.1038/s41598-018-31022-3 . hal-02363288

**HAL Id: hal-02363288**

**<https://hal.science/hal-02363288v1>**

Submitted on 21 Dec 2020

**HAL** is a multi-disciplinary open access archive for the deposit and dissemination of scientific research documents, whether they are published or not. The documents may come from teaching and research institutions in France or abroad, or from public or private research centers.


L'archive ouverte pluridisciplinaire **HAL**, est destinée au dépôt et à la diffusion de documents scientifiques de niveau recherche, publiés ou non, émanant des établissements d'enseignement et de recherche français ou étrangers, des laboratoires publics ou privés.

# SCIENTIFIC REPORTS



OPEN

## Bony pseudoteeth of extinct pelagic birds (Aves, Odontopterygiformes) formed through a response of bone cells to tooth-specific epithelial signals under unique conditions

Antoine Louchart<sup>1,2</sup>, Vivian de Buffrénil<sup>3</sup>, Estelle Bourdon <sup>4,5</sup>, Maitena Dumont<sup>1,6</sup>, Laurent Viriot<sup>1</sup> & Jean-Yves Sire<sup>7</sup>

Modern birds (crown group birds, called Neornithes) are toothless; however, the extinct neornithine Odontopterygiformes possessed bone excrescences (pseudoteeth) which resembled teeth, distributed sequentially by size along jaws. The origin of pseudoteeth is enigmatic, but based on recent evidence, including microanatomical and histological analyses, we propose that conserved odontogenetic pathways most probably regulated the development of pseudodentition. The delayed pseudoteeth growth and epithelium keratinization allowed for the existence of a temporal window during which competent osteoblasts could respond to oral epithelial signaling, in place of the no longer present odontoblasts; thus, bony pseudoteeth developed instead of true teeth. Dynamic morphogenetic fields can explain the particular, sequential size distribution of pseudoteeth along the jaws of these birds. Hence, this appears as a new kind of deep homology, by which ancient odontogenetic developmental processes would have controlled the evolution of pseudodentition, structurally different from a true dentition, but morphologically and functionally similar.

All living birds are edentulous. Fossil representatives of crown group birds (Neornithes) with documented jaw elements indicate that tooth loss occurred between 125 and 66 million years ago (Ma)<sup>1,2</sup>, whereas genomic data point to 116 Ma<sup>3</sup>. However, members of an extinct Neornithine clade known from almost 60 Ma to ca. 2.5 Ma, the order Odontopterygiformes, large pelagic birds, grew a series of pseudoteeth along their jaw tomia, the cores of which were made of bone<sup>4,5</sup> (Fig. 1). The earliest Paleocene Odontopterygiformes already had a pseudodentition<sup>6</sup>. Histologically, the bony cores of these protuberances were a continuity of the supporting jaw, as they consisted of the same kind of bone tissue; therefore, they were merely excrescences of the tomial cortex, with their development starting at the end of the circumferential growth of the jaw bones<sup>5</sup>. Pseudoteeth comprise none of the typical hard tissues that form true teeth (dentin, enamel, cement), and are not inserted in alveoli (sockets) -or grooves. Moreover, the occurrence of numerous neurovascular foramina openings at the surface

<sup>1</sup>CNRS UMR 5242 Institut de Génétique Fonctionnelle de Lyon, Team Evo devo of vertebrate dentition, Université de Lyon, ENS de Lyon, 69364, Lyon cedex, 07, France. <sup>2</sup>Université de Lyon, UCBL, ENSL, CNRS, UMR 5276 LGL-TPE, 69622, Villeurbanne, France. <sup>3</sup>Sorbonne-Universités, Museum National d'Histoire Naturelle, Centre de Recherche sur la Paléobiodiversité et les Paléoenvironnements (CR2P), 75005, Paris, France. <sup>4</sup>The Natural History Museum of Denmark, Section of Biosystematics, DK-2100, Copenhagen, Denmark. <sup>5</sup>Université Pierre et Marie Curie, UMR 7205, Laboratoire Informatique et Systématique, 75005, Paris, France. <sup>6</sup>UMR CNRS/MNHN 7179, "Mécanismes adaptatifs: des organismes aux communautés", 75005, Paris, France. <sup>7</sup>CNRS UMR7138-Evolution Paris-Seine, Institut de Biologie Paris-Seine, Université Pierre et Marie Curie, 75005, Paris, France. Laurent Viriot and Jean-Yves Sire contributed equally. Correspondence and requests for materials should be addressed to A.L. (email: [antoine.louchart@ens-lyon.fr](mailto:antoine.louchart@ens-lyon.fr))

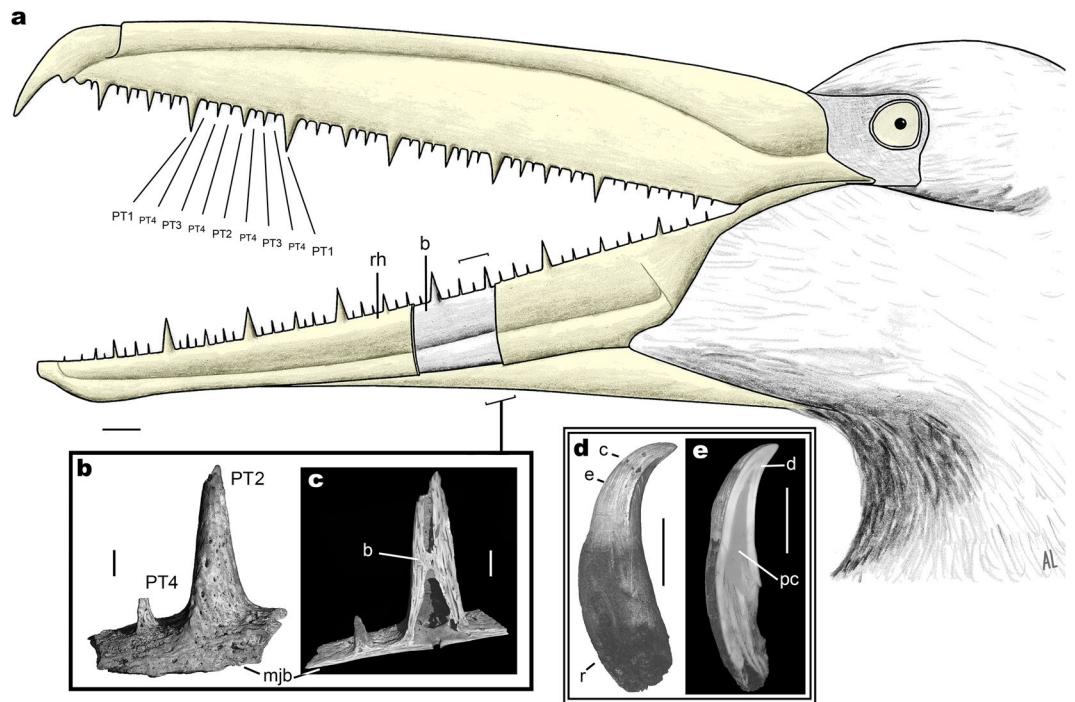


**Figure 1.** Schematic reconstruction of the pseudodentition of a four-ranked pseudotoothed bird. **(a)** Left view of reconstructed beak and head. The rostrum and most of the mandible are represented with the rhamphotheca (keratinized epithelium; in yellow) covering the jaw bones, except for a small area of the mandible to show the underlying bone. **(b)** Magnification of the bony cores of two adjacent pseudoteeth (the larger is a PT2, the smaller is a PT4) of *Pelagornis mauretanicus* (AaO-PT-B)<sup>5</sup>, in lateral x-ray microtomographic view. **(c)** Structure of the pseudoteeth bony cores in **(a)**, shown in parasagittally truncated x-ray microtomographic view. **(d and e)** (double frame), true tooth of the Cretaceous bird *Hesperornis regalis* (YPM.1206B)<sup>22</sup> for comparison with pseudoteeth (in volume and parasagittally truncated synchrotron x-ray microtomographic views, respectively). Proportions based on data from *Pelagornis* species such as *P. mauretanicus*<sup>5</sup>. Views in inserts are reversed, except **(c)**, in order to fit a left mandibular placement in lateral view. The real position (left vs. right, rostral vs. mandibular) of the *P. mauretanicus* pseudoteeth and the *H. regalis* tooth, shown in inserts **(b–e)**, is indeterminate<sup>5,22</sup>. Distribution of PT1s to PT4s is indicated along part of the rostrum. b, bone; c, crown; d, dentin; e, enamel; mjb, main jaw bone; pc, pulp cavity; r, root; rh, rhamphotheca. Scale bars, main frame 2 cm, inserts **(b–e)** 2 mm.

of the pseudoteeth bony cores (Fig. 1) indicates that the latter must have been covered by epithelial sheaths that molded onto their surface<sup>4,5</sup>. These epithelial sheaths are likely to have been keratinized, like the current avian rhamphotheca, albeit relatively late in post-hatching development, suggesting altriciality<sup>5</sup>. The pseudodentition of Odontopterygiformes, strikingly resembles a vertebrate marginal dentition in terms of external morphology (conical, “caniniform” shape), location on jaw tomsia, and regular, serial (meristic) distribution. In addition, pseudodentition is characterized by a very peculiar, serial distribution of the pseudoteeth (Fig. 1), alternating by size along the jaw tomsia, and involving three to five size classes (“ranks”) in adults, depending on species<sup>4,5,7</sup> (see also SFig. 1). Here we have ranked the pseudoteeth from 1 (PT1s, the largest) to 4 and 5 (PT5s, the smallest, existing in at least one species; SFig. 2). These alternations are reminiscent of the “waves” of odontogenetic developments described in reptiles<sup>8–11</sup>. The phylogenetic position of pseudotoothed birds among basal Neornithes is still debated, with the most prominent hypotheses being a sister relationship with either crown Anseriformes<sup>5,12,13</sup>, or crown Galloanserae, or crown Neognathae<sup>13</sup> (Fig. 2).

Until now, the evolutionary and developmental origins of pseudoteeth have been challenging. Nevertheless, by considering the unique characteristics of the pseudodentition, the growth pattern of individual pseudoteeth in one species<sup>5</sup>, as well as new, original lines of evidence, we propose an integrative developmental model which suggests that a diverted odontogenetic potential was probably active (see also Supplementary Text, SText1) in the developmental control of pseudodentition (see also SText 2).

### Late Growth and Rhamphotheca Keratinization

The micro-anatomical and histological characteristics of pseudoteeth bony cores in the odontopterygiform *Pelagornis mauretanicus* indicate that their growth on the jaw tomsia started during, or shortly after, completion of the circumferential (sub-periosteal) growth of the supporting jaw bones (i.e. growth in diameter or thickness of the dentaries, premaxillaries, or maxillaries)<sup>5</sup> (see also SText 3). Such a late pseudoteeth growth would have been associated with delayed keratinization of the overlying epithelial layers long after hatching<sup>5</sup> and just prior to independence from the parents, presumably approaching 18 months after hatching in large pseudotoothed bird species (SText 4). Therefore, until this late keratinization, the whole epithelium would have remained alive

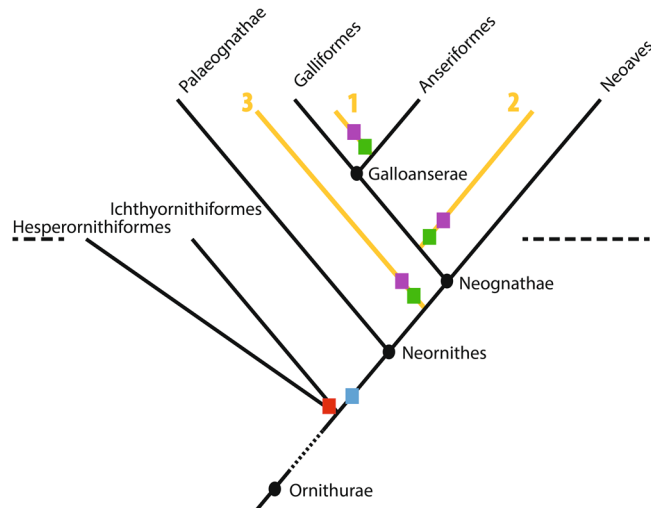


**Figure 2.** Hypotheses for the phylogenetic position of pseudotoothed birds (Odontopterygiformes). The three hypotheses of phylogenetic placement of the Odontopterygiformes are shown in orange: basal within Anseriformes (1), sister to crown Galloanserae (2), or sister to crown Neognathae (3). Squares indicate the probable position of main innovations related to jaws: acquisition of streptognathism and loss of mandibular symphysis (red square in Hesperornithiformes and Ichthyornithiformes, violet squares in Odontopterygiformes), loss of teeth on the line to Neornithes (blue square), and acquisition of pseudoteeth in Odontopterygiformes (green squares). The horizontal dashed line indicates approximate position of the Cretaceous-Paleogene extinction event.

and continued odontogenetic signaling until late development. In contrast, early epithelium keratinization (e.g. *Gallus gallus*) implies the death of epithelial cells across most of the epithelial depth, rendering interaction with the underlying mesenchyme impossible. Such delayed rhamphothecal keratinization might be paralleled by the existence of a soft rhamphotheca, at least locally, in adult representatives of three extant bird taxa: Anseriformes, Apterygidae and some Charadriidae, lineages that have been toothless for a long time<sup>5</sup>. In the hypothesis of a sister relationship between the orders Odontopterygiformes and Anseriformes (superorder Odontoanserae)<sup>12</sup>, a shared phylogenetic background might have favoured the effects of a mutation which caused delayed epithelial keratinization in pseudotoothed birds. Late epithelial keratinization would be viable for young birds if the latter did not use their fragile, acute, growing pseudoteeth with soft epithelium, but were fed by adults during a prolonged period, at least until the end of pseudodentition growth and full rhamphothecal keratinization<sup>5</sup>.

Comparable altriciality is a derived condition in several lineages<sup>14</sup>; however, altriciality in Odontopterygiformes – be it sister to the Neognathae, the Galloanserae or the Anseriformes – would have been the most basally derived altriciality, given that all basal Neornithes (Palaeognathae, Anseriformes, and Galliformes) are precocial to superprecocial<sup>14</sup>. Delayed epithelial keratinization, a condition of prolonged epithelial signaling in pseudotoothed birds, would have been a non-counter-selected by-product of their derived altriciality.

In addition to this potential role for prolonged epithelial signaling, the exclusive location of pseudoteeth on the tomial edges of the jaws, their individualization, and regular spacing that constituted a serial meristic trait, and, to a lesser extent, their simple, almost conical tooth-like shape, suggest that some developmental bases were shared with typical odontogenesis (see also SText 5). We propose that, near the end of the circumferential growth of supporting jaw bones, delayed oral epithelial keratinization allowed basal epithelial cells to continue expressing odontogenetic signaling molecules, to which competent ectomesenchymal cells, such as in extant toothed vertebrates, would have been able to respond. Additionally, we postulate that in the absence of such odontogenetic ectomesenchymal competent cells – a situation which occurs in extant birds<sup>15</sup> the osteoblasts of the jaw bone periosteum did respond; enabling oral epithelium-osteoblast interactions to ensue, which induced the differentiation, growth, and shaping of the pseudoteeth. This scenario raises two issues: (i) the effective continuation of epithelial signaling, and (ii) the possibility for periosteal osteoblasts to interact with the signaling basal epithelial cells.

### Efficient Signaling and Responding Osteoblasts

The possible causes of the loss of capability to form teeth in the neornithine basal lineage are as follows: (i) absence of odontogenetic gene expression, among which the expression of *BMP4* by the oral epithelium is a good candidate<sup>15,16</sup>, (ii) lack of competent ectomesenchymal cells which normally migrate from the neural crests into the oral mesenchyme and differentiate into odontoblasts<sup>17</sup>, (iii) lateral shift of the boundary between the epithelium and the mesenchyme<sup>15</sup>, (iv) diversion of gene function toward the formation of a rhamphotheca and subsequent impossibility for the keratinized epithelium to interact with the mesenchyme<sup>1,2</sup> these possible causes are not mutually exclusive<sup>2</sup>. Nevertheless, the earliest steps of odontogenesis still occur in the chick embryo but the sequence of development stops at embryonic day E5, before the tooth bud stage has been reached. In the *talpid<sup>2</sup>* (*ta<sup>2</sup>*) mutant chicken embryo, dental development continues further with the production of tooth rudiments; however, as this mutation is lethal, this development cannot continue later than E17<sup>15</sup>. These data indicate that odontogenetic

epithelial signaling is maintained and can be reactivated in the chicken upon interaction with competent odontoblasts to form tooth rudiments, as demonstrated by using experimental recombination of chick oral epithelial cells and mouse neural crest-derived cells<sup>17</sup>. We postulate that, in the earliest derived toothless odontopterygiforms (after 50 Myrs length of time, or less, since the ancestral neornithine loss of teeth; Fig. 2) the odontogenetic epithelial signaling was still unaltered: *BMP4* signaling was not inactivated and the basal oral epithelial cells were capable of interacting with mesenchyme-derived cells. Therefore, as teeth did not develop, we assume that competent neural crest-derived ectomesenchymal cells were lacking in the oral mesenchyme, and that odontoblasts could not differentiate in response to epithelial cell signaling. Although the first population of cells originating from the neural crest did presumably contribute to the formation of jaw bones through epithelium-mesenchyme interaction, as in extant birds, the second population of neural crest-derived cells did not differentiate into odontoblasts, contrary to what occurs in toothed taxa<sup>18</sup>. This situation could result from two distinct causes: ectomesenchymal cells did not reach the appropriate jaw region to be able to respond to epithelium signaling, or they were not located in the right place or at the right time (like in extant birds)<sup>17</sup>. Indeed, if these cells had been present, pseudoteeth would have displayed most of the characteristics of true teeth – such as a dentin-like tissue surrounding a pulp cavity and other features – which is not the case. The only alternative hypothesis is that osteoblasts from the jaw periosteum facing the oral epithelium did respond to signaling molecules expressed by the basal oral epithelial cells. This means that periosteal osteoblasts were competent to start such an interaction, and continued until the formation of odontoid excrescences. Indeed, osteoblasts are known to have close evolutionary relationships with odontoblasts<sup>19,20</sup>. Osteoblasts – cells of mesenchymal origin – have strong developmental affinities with odontoblasts of ectomesenchymal origin, as evidenced by numerous examples of toothed vertebrates blurring the limit between bone and dentine with a histological continuum<sup>19</sup>. Alveolar bone first appeared at least in basal amniotes<sup>21</sup>, being identified in a close relative of the last common ancestor of mammals and sauropsids. Hence, both alveolar bone and dentin were present in the Ichthyornithiformes and the Hesperornithiformes, which are the nearest toothed relatives of the Neornithes<sup>22</sup>, and pseudotoothed birds. Both alveolar bone and dentin arise from the same cell population that differentiates into odontoblasts and osteoblasts, respectively; a differentiation process regulated by various genes including *Runx2*<sup>20</sup>. Therefore, we postulate that the periosteal osteoblasts that formed pseudoteeth were capable of responding, with their own potential, to oral epithelial cell signaling.

Another necessary condition for pseudotooth formation in Odontopterygiformes (see SText 6) is that the oral epithelium signaling, and its subsequent interactions with the mesenchyme, continued sufficiently late during ontogeny, ending only when the delayed keratinization of the basal epithelial cells occurred. Indeed, during this period, the jaw bones increased in circumference, which allowed periosteal osteoblasts to interact with the basal epithelial cells due to their close proximity. This necessary time window was made possible relatively late in ontogeny, but nevertheless early enough thanks to prolonged oral epithelium signaling. Based on the known distance of diffusion of the oral epithelial odontogenetic signaling through the mesenchyme in extant toothed taxa, the optimal distance favouring interactions between the basal epithelial cells and the periosteum should be as small as a few tens of micrometers (max. ~100 μm)<sup>23,24</sup>.

### Origin of Shape

Once periosteal osteoblasts had responded to the signaling molecules secreted by the basal cells of the oral epithelium, the genetical cascade controlling epithelial-mesenchymal interactions was initiated, as for normal odontogenesis<sup>25</sup>. Osteoblasts proliferated as meristically individualized populations developing at regularly spaced intervals along the tomial surface of the jaw bones (Figs 3 and 4). Opposite these “pseudotooth primordia”, the basal epithelial cells also proliferated and differentiated into “pre-ameloblasts”, which then developed into dental organs and invaginated as during true tooth development, forming serial bell-like structures. Simultaneously, underneath these, the osteoblasts formed bony cones, the shape of which was controlled by the dental organs (Figs 3 and 4). The conical, caniniform shape of pseudoteeth demonstrates such an “ameloblast”-osteoblast interaction controlling their growth. As the bony cones of the pseudoteeth grew, the dental organs extended, protruding along the external, tomial side. The forming pseudoteeth continued growing until the epithelium started keratinizing and no longer interacting with the osteoblasts, which ceased proliferation and bone formation. The final shape of the pseudoteeth is unicuspid, sub-conical and sharp, though rostro-caudally flattened in lower-ranked (smaller) pseudoteeth (see below), with slight additional features for some of them (ridge, curvature; see STable 1). This process agrees with a general inheritance of the “bell” shape that was presumably present in the closest (and latest) toothed ancestor, judging from the pseudoconical, “caniniform” tooth shape in the sister-taxa of Neornithes, *Ichthyornis* and Hesperornithiformes (notwithstanding the curvature of their rostral-most teeth)<sup>22,26</sup>. It is noteworthy that the “ameloblasts”, although controlling the pseudotooth shape, were unable to deposit enamel matrix proteins on the bone surface. Indeed, all the specific genes encoding these proteins were already invalidated in the earliest Odontopterygiformes, about 50 myrs after the common ancestor of modern birds lost the capability to develop teeth – as they are invalidated in extant birds<sup>27,28</sup>.

The growth of pseudodentition ended after it expressed its unique, alternate distribution of unequally-sized pseudoteeth. The setting of this particular and regular size distributional pattern implies further characterization of our model.

### Origin of Positions

The regular spacing of adjacent PT1s reflects the regulation of a meristic trait. Since the spacing and tomial location of pseudoteeth are identical to those with a true dentition, it suggests a similar process in the setting up of the sites where these meristic structures developed. As hypothesized by several authors for reptilian teeth<sup>9,11,29–31</sup>, the setting up of a serial distribution of the invaginations, where interaction developed, was presumably induced by equally dimensioned and equally-spaced inhibition zones. These morphogenetic fields inhibited the development of another pseudotooth within the radius of a sphere-like zone of influence (Fig. 4). Inhibition is hypothesized

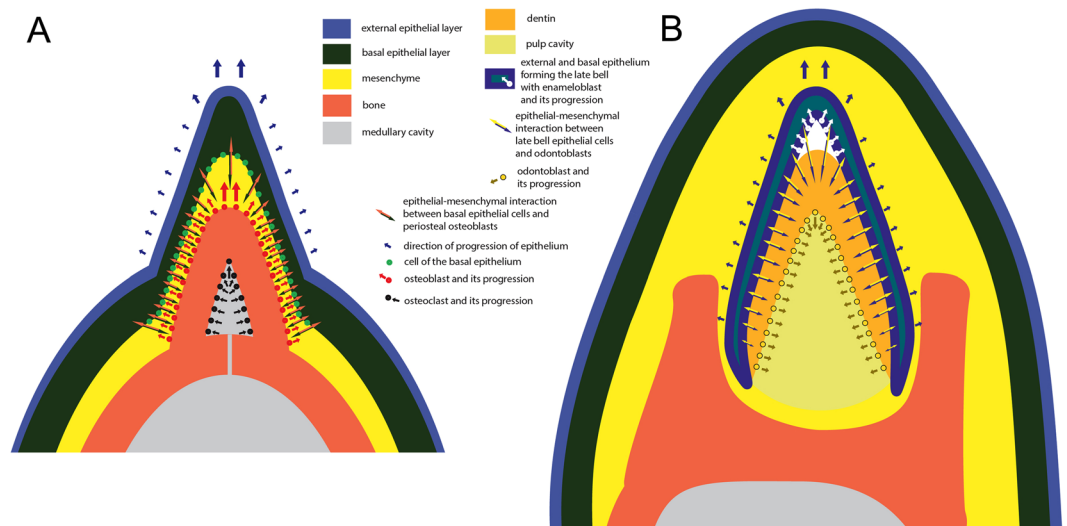


**Figure 3.** Proposed model of pseudotooth development compared with that of a tooth. Schematized transverse jaw section across a pseudotooth (A) and across a true tooth (B). In (A) the developing pseudotooth is shown at a growth stage approximately equivalent to that of stage 6 in Fig. 4. In (B) the developing tooth is shown schematically at “late bell” stage. In both instances epithelial-mesenchymal interactions are indicated, with the different categories of involved tissues, and their direction of growth. Thickness of tissues is exaggerated for convenience of visibility, especially for the mesenchyme.

to have been induced by the action of molecules diffusing from the initial formation centre of each pseudotooth (around the pseudotooth apex), with all inhibition zones being with the same radius of influence. The molecular evidence of such initial inhibitory zones in dentition development, appearing simultaneously with the initially developing tooth germs, has been presented for trout dentition<sup>32</sup>. In mammals, the involved signaling molecules, including *SHH*, *BMP4*, and *FGF8*, are secreted from the epithelium, resulting in a signaling response from the mesenchyme, which in turn induces the odontogenetic potential of the epithelium, prompting the continuing cascade of epithelial-mesenchymal interactions<sup>17</sup>. In birds, a loss of seriality, concomitant with a loss of dentition and the emergence of a continuous rhamphotheca<sup>2</sup>, may correspond to a change in the *SHH* expression, which becomes more broadly expressed in an antero-posterior direction without a gap<sup>33</sup>. The *SHH* expression in Odontopterygiformes might have retained a serial pattern inherited from toothed ancestors, or re-acquired it independently, this regulating gene being otherwise involved in numerous pathways distinct from odontogenesis.

### Inhibition Zones and Size Distribution

Aside from pseudoteeth shape, location, and meristic characteristics – features homologous to a majority of vertebrate dentitions – adult odontopterygiforms display three to five size classes of pseudoteeth arranged in a regular, sequential manner: PT2s are located midway between two consecutive PT1s, PT3s are located between PT1s and PT2s, PT4s (if present, depending on species) are situated between PT3s and PT2s and between PT3s and PT1s (Fig. 1, STable 1); tiny intervening PT5s were observed here in only one case (SFig. 2).

The hypothetical causes of the sequential size distribution of equally-spaced pseudoteeth, which can be formalized as a series of pseudoteeth, PT1-(5)-(4)-(5)-3-(5)-(4)-(5)-2-(5)-(4)-(5)-3-(5)-(4)-(5)-1 (Fig. 1), can be classified as four (not strictly exclusive) modes of growth: (i) synchronous start of the growth of PTs, of all ranks, and their differential growth rates; (ii) synchronous start and asynchronous end; (iii) asynchronous start and synchronous end. A last hypothesis (iv) would be that an asynchronous start of growth (later start for smaller pseudoteeth) would indirectly derive from a simultaneous elongation of supporting jaw bones, resulting in an increase of the distance between two adjacent large PTs, and providing a new space with minimal growth inhibition midway between these. However, there is no evidence of an increase in intervals when comparing juvenile odontopterygiform fossils with adults (SText7); therefore hypothesis (iv) can be discarded. Indeed, just prior to pseudotooth growth, the circumference of the jaw bones was fully grown, and any elongation could only have occurred at their rostral and caudal ends. Hypothesis (i) – involving different growth speeds in pseudoteeth of different ranks – has also been dismissed, as no such differences can be inferred from paleohistology<sup>5</sup>. Juvenile fossil jaws show faint bumps at the location of the future, adult pseudoteeth of lower ranks (see SText 7; SFig. 2), indicating that the latter started developing much later than higher-ranked (larger) ones. This observation supports hypothesis (iii), i.e. asynchronous start of growth and synchronous end, as opposed to hypothesis (ii).

In the framework of an asynchronous start and a synchronous end of pseudoteeth growth, we propose that the dynamic action of inhibition zones controlled the differential starts of growth, and therefore the final relative sizes of the differently ranked pseudoteeth.

Once inhibition zones were established with the first developing PT1s, determining seriality, they continued to control and limit the growth of adjacent pseudoteeth. This dynamic process caused the inhibition zones to decrease in radius through developmental time, as proposed earlier for reptilian tooth formation<sup>11,29,30</sup>. Likewise,

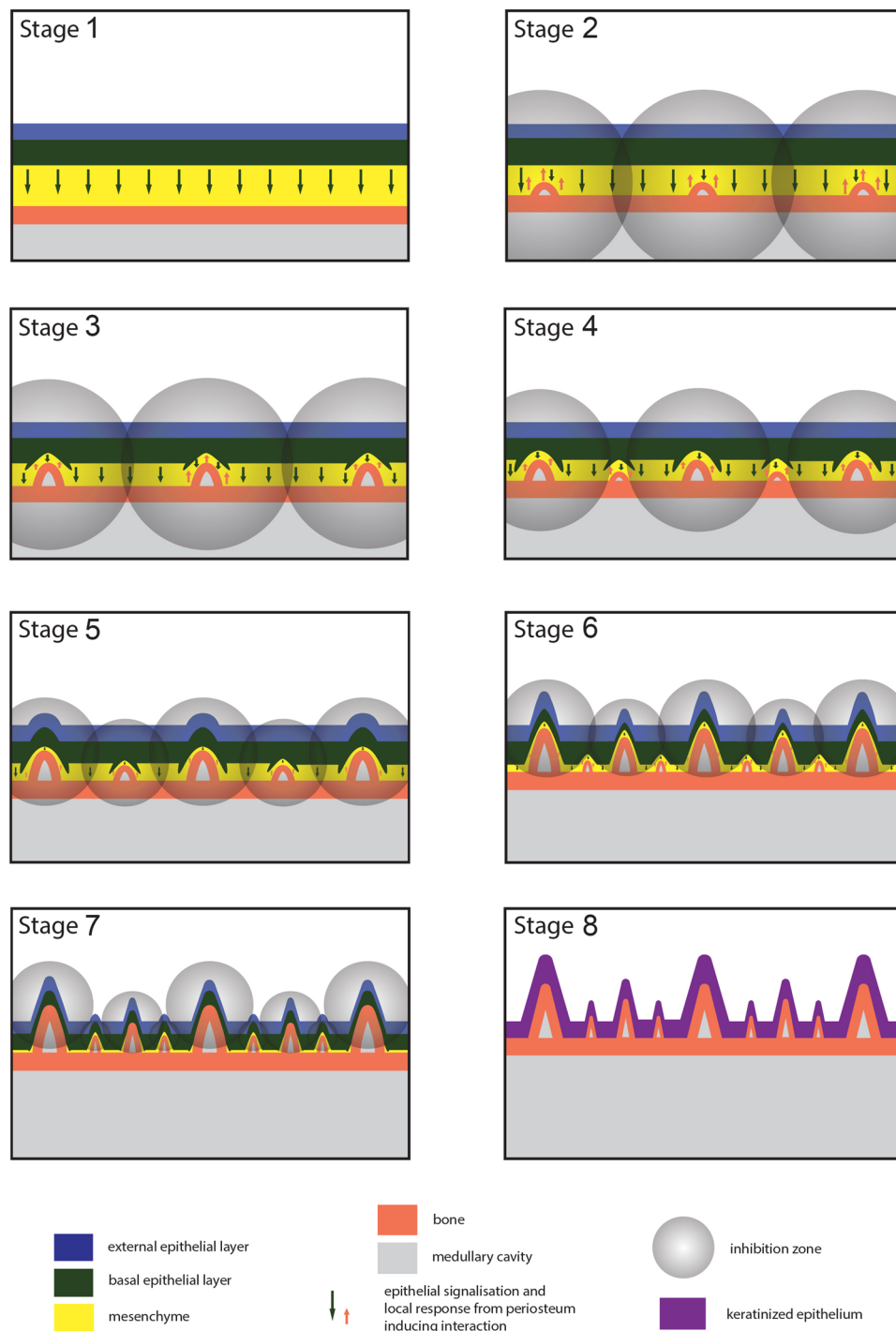


**Figure 4.** Proposed model of pseudodentition development. The differential growth of the differently ranked pseudoteeth is shown in eight stages, in the parasagittal section of a jaw for all pseudoteeth. For convenience of visibility, tissue thicknesses are exaggerated,  $\sim 10 \times$  (bone, epithelium) and  $\sim 100 \times$  (mesenchyme). Epithelial-mesenchymal interactions between the basal epithelium cells and the periosteal osteoblasts start when the intervening space becomes lower than  $\sim 100 \mu\text{m}$  (Stage 2). This interaction ends when epithelial cells become keratinized (Stage 8).

but on a smaller scale, inhibition zones among cusps in a single tooth are known to originate from enamel knots, in some mammals, and to contribute to the regulation of the development of adjacent, secondary enamel knots of ultimately smaller cusps<sup>34</sup>.

As soon as the almost conical pseudoteeth started to grow, zones of inhibition would have set up in the form of spheres of molecular influence, centered on the apex (equivalent to the enamel knot of developing vertebrate teeth<sup>25,35</sup>) of the invaginating basal epithelial layer. These putatively sphere-like zones of inhibition prevented the

development of adjacent pseudoteeth within their field of influence. While the first series of pseudoteeth were developing (future PT1s), their respective inhibition zones were progressively decreasing in radius. As a consequence, spaces became free from inhibition at locations equidistant from two consecutive PT1s. The PT2 series could then start developing through epithelial-osteoblast interactions, which in turn produced their own smaller inhibition zone (Fig. 4). This process could also occur later in development so that PT3s could start growing between PT1s and PT2s (Fig. 4), inducing their own, even smaller inhibition zone. Further on, a fourth (and fifth) series could start growing in species bearing four-ranked (and five-ranked) pseudodentitions. Pseudoteeth emerged progressively (largest first) as excrescences of the tomia, formed by bone and covered by epithelium. The final developmental stage of the pseudodentition saw each pseudotooth attain its definitive size, presumably consecutive to rapid epithelial keratinization. This fast but late epithelial keratinization might have been genetically programmed; alternatively, we suggest that it could have resulted from an epigenetic cause. The start of mechanically using the beak tomia by the young at the end of the altricial period would have initiated the keratinization process – local mechanical stress is known to induce keratinization<sup>36</sup> – which would have proceeded from the external to the basal layer of the oral epithelium, finally stopping interaction and pseudotooth growth.

Most differences in the size distribution of pseudoteeth across various odontopterygiform species (or unnamed specimens) can be interpreted in terms of the species-specific characteristics of inhibition zones, and their modifications during development (SText 8, STable 1). Nevertheless, a consistent correlation emerges and adds support to our model. In species with a larger interval between PT1s (and/or smaller PT1s), the PT3s show an attenuated size decrease relative to PT2s, compared with the size decrease of PT2s vs PT1s (SText 8). This is what would be expected if the inhibitory action of the larger pseudoteeth actually delayed the growth of the last emerging (lower-ranked/smaller) pseudoteeth – the latter reaching a size limited by the duration of inhibition by the larger pseudoteeth through pseudodentition growth. This duration of inhibition, in our model, is greater with larger PT1s and/or with a smaller interval between them. Another characteristic, common to all taxa, is that the lower-ranked pseudoteeth are increasingly more constricted rostro-caudally. This strongly suggests that increasingly constraining inhibition zones during the development of the lower-ranked pseudoteeth, with a smaller intervening space, imposed narrower spaces for rostro-caudal development. This can be clearly seen in the *Pelagornis* species, where the PT4s are blade-like (when present) (SText 9; S Figs 3 and 4). Aside from the normal features of pseudodentitions and interspecific differences, irregularities often occurred within particular specimens. The causes of these irregularities are often blurred by other sources of variation, such as consistently wider spacings, and larger pseudoteeth at the mid-length of the jaw rather than towards the rostral or caudal extremities (SText 10). In certain circumstances, however, morphogenetic interpretations can be proposed; for instance, in the comparison of the right and left jaw areas of a single specimen, at the same level, with one side differing from the other in terms of spacing. Such an example shows that a larger space between two pseudoteeth corresponds to a larger intervening pseudotooth (SText 11; S Fig. 4) and provides some support to our hypothesis of dynamic inhibition zones, where a wider space allowed either more numerous or larger pseudoteeth.

The particular sequential size distribution of pseudoteeth is paralleled by that of teeth in the dentition of several fish lineages (e.g. in the jaw dentition of the characiforms Cynodontidae and Erythrinidae, and the teeth of the ‘saw’ in the sawsharks of the genus *Pristiophorus*; S Figs 5 and 6). These similarities in size distribution, between these dentitions and pseudodentitions, suggest that they shared a developmental mechanism of differential growth regulation via inhibition zones; a comparison that holds with the setting up of the first dentition in *Pristiophorus* (though not during its subsequent tooth replacements)<sup>37,38</sup>. In the longnose sawshark, *P. cirratus*, the largest teeth grow first, followed by the medium-sized ones, and finally the smaller ones<sup>37–39</sup>, which is similar to the growth sequence considered in our model for pseudodentition. These observations add further support to our hypothesis, since they attest to a possible common underlying mechanism operating on true teeth as well as on pseudoteeth.

### Pseudodentition Deep Homology with Dentition, and Co-Adaptation with Unique Mandibular Characters

Pseudoteeth differ from true teeth, not only in the tissues involved (bone and keratinizing epithelium vs dentin and enamel) and the lack of pulp cavity, but also in their growth and mineralization dynamics, and in relation to the jaw bone. In true teeth, dental tissues develop and mineralize centripetally before attachment to the jaw bone, and once their final shape is achieved the covering tissue deposited by the ameloblasts (enamel) is highly mineralized prior to eruption. In contrast, the bony cores of pseudoteeth were already part of the jaw bone, and they developed and mineralized centrifugally, through a combined process of external accretion and internal resorption of the cortex. The epithelium covering the bony cores of the pseudoteeth became hardened by means of keratinization (like the rest of the rhamphotheca) after ‘eruption’ (emergence) and completed growth. Therefore, in the model we propose, the only common process when comparing pseudotooth and true tooth formation consists of the epithelial-mesenchymal interactions modeling the final shape, and the capability of osteoblasts to respond to epithelial signaling, as odontoblasts do for teeth. This behaviour is made possible by (i) the common evolutionary origin of osteoblasts and odontoblasts, and (ii) the close vicinity of the interacting cells, osteoblasts, and basal layer epithelial cells. This genetic cascade regulates relatively simple shape, differential growth, and seriality along the tomia. Such an opportunistic diversion of available epithelial odontogenetic signaling making the regulation of bone growth possible is unique among vertebrates. This attests to the considerable plasticity of a developmental program, which is capable in forming highly derived structures similar to dentition, despite the loss of ability to develop true teeth, in crown group birds. As such, this evolutionary innovation not only produced organs that were functionally convergent with dentitions, but is also a new illustration of a kind of deep homology<sup>40</sup>. Future epithelium-mesenchyme recombination experiments might be a mean of testing the model presented here, but previous attempts were not conclusive, due in particular to extremely difficult separation between these two tissues<sup>41</sup>. On the other hand, current knowledge on genic cascades implied in tooth



initiation in mice<sup>42</sup> makes it possible to envision experiments involving beads, impregnated with corresponding epithelium-mesenchyme signaling molecules. These beads would be implanted (*in vivo* or *ex vivo*) between chick embryo oral epithelial and mesenchymal tissues.

Once the process of pseudodontition growth was acquired by an ancestral odontopterygiform, it was maintained in derived lineages presumably for adaptive reasons (see also SText 12). Among Ornithurae, the combination of streptognathism and absence of mandibular symphysis only occurs in the Odontopterygiformes and the Cretaceous toothed avian taxa Ichthyornithiformes and Hesperornithiformes, the respective sister taxa of crown group birds<sup>5,43</sup>. This conformation weakened grasping strength<sup>5,43</sup> and, in the absence of teeth in odontopterygiforms, pseudodontition could have acted as a counterbalancing grasping enhancer. The conformation of the mandible would have evolved in co-adaptation with the pseudodontition. This evolutionary resourcefulness produced structures possibly less resistant than teeth<sup>44</sup>. Nevertheless, pseudotoothed birds were extremely successful, wandering the world's oceans for more than 55 million years<sup>6,7</sup>.

## Methods

**Observations and X-ray microtomography.** Specimens of *Dasornis* (Paleocene-Eocene, Morocco)<sup>6</sup> and *Pelagornis* (Pliocene, Morocco)<sup>5</sup> were examined for comparison, as well as specimens of *Hesperornis regalis* (late Cretaceous, North America)<sup>22</sup>. The *Dasornis* and *Pelagornis* fossils were imaged using conventional X-ray microtomography, performed at the Ecole Normale Supérieure de Lyon and at General Electrics (Lyon) using Phoenix Nanotom. The *Hesperornis* fossil was imaged using synchrotron X-ray microtomography at the European Synchrotron Radiation Facility (Grenoble). The 3D volumes obtained were analyzed using VGStudio MAX 2, as previously described<sup>5,22</sup>.

**Data availability.** Data analysed during this study are included as Supplementary Information files. Any additional data are available from the author upon reasonable request.

## References

- Davit-Béal, T., Tucker, A. & Sire, J. Y. The loss of ability to form teeth and enamel in living tetrapod taxa: genetic data and morphological adaptations. *J. Anat.* **214**, 477–501 (2009).
- Louchart, A. & Viriot, L. From snout to beak: the loss of teeth in birds. *Trends Ecol. Evol.* **26**, 663–673 (2011).
- Meredith, R. W., Zhang, G., Gilbert, M. T. P., Jarvis, E. D. & Springer, M. S. Evidence for a single loss of mineralized teeth in the common avian ancestor. *Science* **346**, 1254390 (2014).
- Howard, H. A gigantic “toothed” marine bird from the Miocene of California. *Bull. Dept Geol. Santa Barbara Mus. Nat. Hist.* **1**, 1–23 (1957).
- Louchart, A. *et al.* Structure and growth pattern of pseudoteeth in *Pelagornis mauretanicus* (Aves, Odontopterygiformes, Pelagornithidae). *PLoS ONE* **8**, e80372 (2013).
- Bourdon, E., Amaghazaz, M. & Bouya, B. Pseudotoothed birds (Aves, Odontopterygiformes) from the Early Tertiary of Morocco. *Am. Mus. Novit.* **3704**, 1–71 (2010).
- Mourer-Chauviré, C. & Geraads, D. The Struthionidae and Pelagornithidae (Aves: Struthioniformes, Odontopterygiformes) from the late Pliocene of Ahl Al Oughlam, Morocco. *Oryctos* **7**, 169–194 (2008).
- Edmund, A. G. Tooth replacement phenomena in the lower vertebrates. *Roy. Ont. Mus. Life Sci. Div. Contr.* **52**, 1–190 (1960).
- Edmund, A. G. In *Biology of the Reptilia*, vol. 1 (eds Gans, C., Bellairs, A. dA. & Parsons, T. S.) 117–200 (Academic Press, 1969).
- Osborn, J. W. New approach to Zahnreihen. *Nature* **225**, 343–346 (1970).
- Osborn, J. W. The ontogeny of tooth succession in *Lacerta vivipara* Jacquin (1787). *Proc. R. Soc. Lond. B.* **179**, 261–289 (1971).
- Bourdon, E. Osteological evidence for sister group relationship between pseudo-toothed birds (Aves: Odontopterygiformes) and waterfowls (Anseriformes). *Naturwissenschaften* **92**, 586–591 (2005).
- Mayr, G. Cenozoic mystery birds – on the phylogenetic affinities of bony-toothed birds (Pelagornithidae). *Zool. Scr.* **40**, 448–467 (2011).
- Starck, J. M. & Ricklefs, R. E. In *Avian Growth and Development: Evolution within the Altricial-Precocial Spectrum* (eds Starck, J. M. & Ricklefs, R. E.) 3–30 (Oxford University Press, 1998).
- Harris, M. P., Hasso, S. M., Ferguson, M. W. J. & Fallon, J. F. The development of archosaurian first-generation teeth in a chicken mutant. *Curr. Biol.* **16**, 371–377 (2006).
- Chen, Y. *et al.* Conservation of early odontogenetic signaling pathways in Aves. *Proc. Natl Acad. Sci. USA* **97**, 10044–10049 (2000).
- Mitsiadis, T. A., Caton, J. & Cobourne, M. Waking-up the sleeping beauty: recovery of the ancestral bird odontogenic program. *J. Exp. Zool. (Mol. Dev. Evol.)* **306B**, 227–233 (2006).
- Schneider, R. A. & Helms, J. A. The cellular and molecular origins of beak morphology. *Science* **299**, 565–568 (2003).
- Hall, B. K. & Witten, P. E. In *Major Transitions in Vertebrate Evolution* (eds Anderson, J. S. & Sues, H. D.) 13–56 (Indiana University Press, 2007).
- Komori, T. Regulation of bone development and extracellular matrix protein genes by RUNX2. *Cell Tissue Res.* **339**, 189–195 (2010).
- LeBlanc, A. R. H. & Reisz, R. R. Periodontal ligament, cementum, and alveolar bone in the oldest herbivorous tetrapods, and their evolutionary significance. *PLoS ONE* **8**, e74697 (2013).
- Dumont, M. *et al.* Synchrotron imaging of dentition provides insights into the biology of *Hesperornis* and *Ichthyornis*, the “last” toothed birds. *BMC Evol. Biol.* **16**, 178 (2016).
- Jessel, T. M. & Melton, D. A. Diffusible factors in vertebrate embryonic induction. *Cell* **68**, 257–270 (1992).
- Vainio, S., Karavanova, I., Jowett, A. & Thesleff, I. Identification of *BMP-4* as a signal mediating secondary induction between epithelial and mesenchymal tissues during early tooth development. *Cell* **75**, 45–58 (1993).
- Thesleff, I. Epithelial-mesenchymal signalling regulating tooth morphogenesis. *J. Cell Sci.* **116**, 1647–1648 (2003).
- Martin, L. D. & Stewart, J. D. Teeth in *Ichthyornis* (Class: Aves). *Science* **195**, 1331–1332 (1977).
- Sire, J. Y., Delgado, S. C. & Girondot, M. Hen's teeth with enamel cap: from dream to impossibility. *BMC Evol. Biol.* **8**, 246 (2008).
- Al-Hashimi, N., Lafont, A. G., Delgado, S., Kawasaki, K. & Sire, J. Y. The enamel genes in lizard, crocodile, and frog and the pseudogene in the chicken provide new insights on enamel evolution in tetrapods. *Mol. Biol. Evol.* **27**, 2078–2094 (2010).
- Osborn, J. W. The interpretation of patterns in dentitions. *Biol. J. Linn. Soc.* **9**, 217–229 (1977).
- Osborn, J. W. Relationship between growth and the pattern of tooth initiation in alligator embryos. *J. Dent. Res.* **77**, 1730–1738 (1998).
- Westergaard, B. & Ferguson, M. W. J. Development of the dentition in *Alligator mississippiensis*: upper jaw dental and craniofacial development in embryos, hatchlings, and young juveniles, with a comparison to lower jaw development. *Am. J. Anat.* **187**, 393–421 (1990).

32. Fraser, G. J., Graham, A. & Smith, M. M. Developmental and evolutionary origins of the vertebrate dentition: molecular controls for spatio-temporal organisation of tooth sites in osteichthyans. *J. Exp. Zool. (Mol. Dev. Evol.)* **306B**, 183–203 (2006).
33. Tokita, M., Chaeychomsri, W. & Siruntawinetti, J. Developmental basis of toothlessness in turtles: insight into convergent evolution of vertebrate morphology. *Evolution* **67**, 260–273 (2012).
34. Salazar-Ciudad, I. & Jernvall, J. A computational model of teeth and the developmental origins of morphological variation. *Nature* **464**, 583–586 (2010).
35. Westergaard, B. & Ferguson, M. W. J. Development of the dentition in *Alligator mississippiensis*. Early embryonic development in the lower jaw. *J. Zool.* **210**, 575–597 (1986).
36. Bragulla, H. H. & Homberger, D. G. Structure and functions of keratin proteins in simple, stratified, keratinized and cornified epithelia. *J. Anat.* **214**, 516–559 (2009).
37. Slaughter, B. H. & Springer, S. The replacement of rostral teeth in sawfishes and sawsharks. *Copeia* **1968**, 499–506 (1968).
38. Welten, M., Smith, M. M., Underwood, C. & Johanson, Z. Evolutionary origins and development of saw-teeth on the sawfish and sawshark rostrum (Elasmobranchii; Chondrichthyes). *R. Soc. Open sci.* **2**, 150189 (2015).
39. Gudger, E. W. How difficult parturition in certain viviparous sharks and rays is overcome. *Obstet. Gynecol. Surv.* **7**, 202–210 (1952).
40. Shubin, N., Tabin, C. & Carroll, S. Deep homology and the origins of evolutionary novelty. *Nature* **457**, 818–823 (2009).
41. Mitsiadis, T. A., Chéraud, Y., Sharpe, P. & Fontaine-Péru, J. Development of teeth in chick embryos after mouse neural crest transplantations. *Proc. Natl Acad. Sci. USA* **100**, 6541–6545 (2003).
42. Mitsiadis, T. A. & Smith, M. M. How do genes make teeth to order through development? *J. Exp. Zool. (Mol. Dev. Evol.)* **306B**, 177–182 (2006).
43. Zusi, R. L. & Warheit, K. I. On the evolution of intraramal mandibular joints in pseudodontorns (Aves: Odontopterygia). *Nat. Hist. Mus. Los Angeles Cnty Sci. Ser.* **36**, 351–360 (1992).
44. Olson, S. L. In *Avian Biology* (eds Farner, D. S., King, J. R. & Parkes, K. C.) 79–252 (Academic Press, 1985).

## Acknowledgements

Funding for AL came from the Agence Nationale de la Recherche, programme Jeune chercheur 'PIAFS', ANR-11-JSV7-004-01 (France), and from the European Synchrotron Radiation Facility proposal funding EC-944 (France). We thank Jill Cucchi for improving and editing the english.

## Author Contributions

A.L. and J.Y.S. conceived the study. E.B. provided fossil material of *Dasornis*. A.L., with primary assistance from J.Y.S., performed the analyses and wrote early drafts of the paper, benefiting from input and discussions with V.d.B., M.D. and L.V. The figures were prepared by A.L., with assistance from M.D. and J.Y.S. The study was supervised by L.V. and J.Y.S. All authors developed and discussed interpretations and conclusions, and participated in preparation of the manuscript.

## Additional Information

**Supplementary information** accompanies this paper at <https://doi.org/10.1038/s41598-018-31022-3>.

**Competing Interests:** The authors declare no competing interests.

**Publisher's note:** Springer Nature remains neutral with regard to jurisdictional claims in published maps and institutional affiliations.



**Open Access** This article is licensed under a Creative Commons Attribution 4.0 International License, which permits use, sharing, adaptation, distribution and reproduction in any medium or format, as long as you give appropriate credit to the original author(s) and the source, provide a link to the Creative Commons license, and indicate if changes were made. The images or other third party material in this article are included in the article's Creative Commons license, unless indicated otherwise in a credit line to the material. If material is not included in the article's Creative Commons license and your intended use is not permitted by statutory regulation or exceeds the permitted use, you will need to obtain permission directly from the copyright holder. To view a copy of this license, visit <http://creativecommons.org/licenses/by/4.0/>.

© The Author(s) 2018

## **Supplementary Information accompanying Louchart et al. “Bony pseudoteeth of extinct pelagic birds (Aves, Odontopterygiformes) formed through a response of bone cells to tooth-specific epithelial signals under unique conditions”**

Antoine Louchart, Vivian de Buffrénil, Estelle Bourdon, Maïtena Dumont, Laurent Viriot and Jean-Yves Sire

### **Supplementary text**

#### **Supplementary Discussion, section 1. Alternative developmental models would not be consistent with data.**

The only alternative developmental model incorporating elements of analogy or homology with support from extant organisms (other than the model we propose in the main text), would be the development of spurs on the legs of some galliform birds and cassowaries<sup>1</sup>, with additional examples of similar spurs on the carpometacarpi or metacarpi in other diverse avian taxa<sup>1-3</sup>. The development of the tarsometatarsal (leg) spurs has already been investigated<sup>4-6</sup>, and like pseudoteeth these spurs consist of pseudoconical bony cores covered with a keratinous sheath, which is acute in several species. In a few species, these leg spurs have a meristic distribution, i.e. several spurs are present on each tarsometatarsus and are evenly spaced along the tarsometatarsus shaft<sup>7</sup>. Developmentally, however, the keratinous sheaths of the leg spurs grow and become hardened before the spurs bony cores form. The condensation of the spur's bony core starts just as the bone separates from the tarsometatarsus, inside the forming spur sheath, near its apex – away from the almost fully grown tarsometatarsus shaft<sup>4,5,8</sup>. The osteoblasts located at the base of the spur bone then interact with the periosteal osteoblasts at the surface of the tarsometatarsal shaft, and both surfaces (spur bone base and adjacent tarsometatarsus surface) join together through limited osteoblast proliferation<sup>4-6,8,9</sup>. Spur bone is secondarily fused to the tarsometatarsus shaft surface; a process which leaves obvious marks at their junction<sup>4,5,8</sup>. Therefore, spur and tarsometatarsus bones initially develop from separate condensations and grow independently until an advanced stage<sup>4,5,8,10</sup>. In contrast, the bony cores of pseudoteeth are excrescences of the jaw bone periosteum by means of osteoblast proliferation; a process which is activated through interactions with the basal layer of the epithelial cells that are not yet keratinized.<sup>11</sup>

#### **Supplementary Discussion, section 2. Pseudodentition is characterized by the unique size distribution and acute shape of pseudoteeth, compared with bony “odontoids” in other vertebrates.**

Bony odontoids in place of teeth constitute a rare feature in vertebrates. In birds, apart from the Odontopterygiformes, they are known only in the extinct insular moa-nalo (flightless giant ducks from the Hawaiian Islands) of the genera *Thambetochea* and *Ptaiochea*<sup>12</sup>. Moa-nalo odontoids resemble the equally-sized thick lamellae of extant geese rhamphothecae. In several anuran lineages, bony odontoids range from fangs to paired bumps<sup>13,14</sup>. The teleost fish *Danionella dracula* exhibits bony fangs and a series of small odontoids<sup>15</sup>. Bony odontoids are also known from several chelonian lineages<sup>16</sup>. The single, symphyseal bony odontoid described in the mandible of an istiodactyl pterosaur, also called a pseudotooth<sup>17</sup>, does not actually resemble the odontopterygiform pseudoteeth, the latter forming paired series in both mandible and rostrum. None of these examples resemble the large acute odontopterygiform pseudoteeth, which resemble teeth of a jaw's normal dentition and exhibit a particular, regular and sequential size distribution. Therefore, we have restricted the use of the terms

pseudotooth and pseudodentition to the Odontopterygiformes. Differences in shape between the bony pseudodentition and its horny cover (i.e. the rhamphotheca covering the jaw bone) might have existed, due to putative variations in rhamphothecal thickness (unknown because it is not preserved during fossilization) according to the size of the pseudotooth bony core covered. The larger pseudoteeth (PT1s and PT2s) had an acute rhamphothecal cover (at least as acute as their bony cores), as shown by the corresponding holes for mandibular PT1s and PT2s, located on the ventral side of the bony rostrum in sufficiently complete specimens<sup>18,19</sup>. Mandibular PT1s and PT2s interlocked into these rostral holes when the jaws were closed. Based on observations on extant large-beaked birds<sup>20</sup>, rhamphothecal thickness in pseudotoothed birds probably ranged from 0.5 mm (over most of the jaw) to a few millimetres in certain regions (e.g. tomial edges, beak tip), perhaps 1-2 mm over the pseudotooth bony cores. Many other birds show serrations on the beak tomia, but these serrations are obtuse and reduced in size – a few millimetres at the most in geese; they are equally sized along the jaws, and exclusively affect the rhamphotheca rather than the underlying bone<sup>1,21</sup>.

### **Supplementary Discussion, section 3. Ontogenetic differences between “tomial teeth” and pseudoteeth.**

The two paired “tomial teeth” reported in the cranial extremity of the rostrum in *Pelagornis orri*<sup>22</sup> and *P. chilensis*<sup>19,23</sup> are extremely similar, and perhaps homologous to the two paired tomial teeth of the extant *Harpagus bidentatus* (Accipitridae; phylogenetically distant from pseudotoothed birds) (SFig. 1). These structures are (i) located exclusively at the rostral (anterior) end of the rostrum, (ii) obtuse and rounded in outline, and (iii) latero-medially flattened unlike pseudoteeth. Tomia are generally blade-shaped like tomial teeth, whereas pseudoteeth, with their much wider base, require a latero-medial widening of the underlying jaw tomia. Tomial teeth are not homologous to pseudoteeth, but they might deserve further investigation with respect to a wider category of “odontoids” in birds. In contrast to pseudoteeth, “tomial teeth” presumably grow synchronously with the main jaw bone. In *P. sandersi* only a single paired rostral tomial tooth is reported<sup>24</sup>, but the above interpretation also applies to that species. Several extant avian taxa aside from *H. bidentatus* exhibit double or simple paired tomial teeth<sup>21</sup>.

### **Supplementary Discussion, section 4. Estimation of the post-hatching growth timing of the beak and pseudodentition in pseudotoothed birds.**

Extant albatrosses (Procellariiformes, Diomedidae) provide interesting elements for estimating the plausible timing of beak growth in pseudotoothed birds, because (i) both taxa share morphological (skeletal) characteristics corresponding to similar adaptations for pelagic foraging, (ii) pseudotoothed birds were most probably altricial in development like albatrosses, and (iii) albatrosses are the largest pelagic seabirds, approaching medium species of Odontopterygiformes in size. In the albatross *Diomedea chrysostoma* (2.20 m wingspan), the definitive beak (culmen) length is reached ca. 100-110 days after hatching<sup>25</sup>. In the same species, fledging (independence of young from parents, which means first use of pseudodentition for catching prey) occurs at 140-150 days after hatching. In the smaller *Calonectris diomedea*, a shearwater (Procellariiformes, Procellariidae; 1.20 m wingspan), adult beak (culmen) length is reached at ca. 60 days, and the adult beak height earlier (like in “long” beaked birds in general) at ca. 35-40 days. Fledging occurs at 95 days (on average) after hatching<sup>26</sup>. Hence, in the shearwater there is a period of ca. 60 days between the end of beak growth in height (i.e. circumference) and independence. Even in the albatross, adult beak height is reached before adult length. There is already a period of 40 days between complete growth in beak length and independence, and perhaps up to 70 days might be inferred between the end of circumferential growth and independence, i.e. ca. 40 % of fledging time.

In the largest albatross *D. exulans* (wingspan over 3 m), fledging occurs at ca. 270 days (nine months) after hatching. Using the relation between its fledging time and body size (and wingspan in these birds) an extrapolation can be attempted in *Pelagornis mauretanicus*, with a wingspan of over 5 m<sup>27</sup>, where fledging might have occurred more than one year after hatching, probably around 18 months. If this time span amounted to 40% (like in *D. chrysostoma*), it would roughly indicate that eight months elapsed in this pseudotoothed bird between completion of circumferential growth of beak (i.e. start of pseudoteeth growth) and independence (i.e. end of keratinization of the rhamphotheca, at the end of pseudoteeth growth). Such an estimate for pseudoteeth growth duration is coherent with our growth model and histological observations<sup>11</sup>.

**Supplementary Discussion, section 5. Evaluating the pertinence of comparison between pseudoteeth and first generation archosaurian teeth, or *talpid2* chicken teeth rudiments with regards to pseudotooth development.**

The purported, superficial resemblance of pseudoteeth with (i) first generation teeth in archosaurians and (ii) tooth rudiments in *talpid2* chicken mutant embryos<sup>28</sup>, has led in the past to suggestions of some level of homology between the development of pseudoteeth and true teeth<sup>19,29,30</sup>. This argumentation, however, is questionable, and not relevant for understanding pseudotooth development. Pseudoteeth differ intrinsically from avian teeth, which are composed of dentin, cement (at least in some taxa), and an enamel crown cover, like most teeth<sup>31</sup>, whereas pseudoteeth are composed of bone and a rhamphothecal cover<sup>11,29,32,33</sup> (incidentally, teeth are not “covered by dentine” *contra* Mayr and Rubilar<sup>19</sup>). Nevertheless, it was suggested that tooth-specific developmental programs might be responsible for pseudotooth development, based on their putative resemblance with the early developmental stages of first-generation archosaurian teeth<sup>19</sup>. However, these earliest “surface teeth” stages are not mere outgrowths of the jaw bone (*contra* Mayr and Rubilar<sup>19</sup>), but projections of the epithelium<sup>34</sup>, in which mesenchyme-derived odontoblast precursors differentiate and form dentin<sup>35</sup>. These teeth are not made of bone and are situated far from the jaw bone; later generation teeth develop deeper into the mesenchyme, from a dental lamina, and only later elongate to fuse with the jaw bone into alveoli<sup>34,35</sup>. Therefore, there is no complete or direct homology (*contra* Mayr and Rubilar<sup>19</sup> and Mayr and Zvonok<sup>30</sup>) between pseudoteeth, which are bony outgrowths at the jaw bone’s surface, and first-generation teeth in archosaurians (and presumably tooth rudiments in *talpid2* chicken mutants)<sup>28</sup>, that are early tooth precursors situated far from the jaw bone with a mesenchymal component made of dentin (predentin in *talpid2* mutant embryos at ca. 17 days)<sup>21</sup>. Therefore, the composition and precise location of pseudoteeth differ radically from those of first generation teeth in archosaurians as well as the tooth rudiments of *talpid2* embryos. The latter two structures do not illustrate any developmental link between pseudoteeth and teeth. In contrast, we have based our model on the general location, seriality and sequential size distribution of pseudoteeth (see Supplementary table STable 1), their shape and growth timing<sup>11</sup>, plus several other independent lines of evidence (present study; see Main text).

**Supplementary Discussion, section 6. Other categories of avian odontoids arose independently, even though a common background for Odontoanserae might be at stake.**

The only other birds that possess bony odontoids on the jaws (the extinct Hawaiian moa-nalo of the genera *Thambetochen* and *Ptaiochen*)<sup>12</sup>, albeit much less developed and acute than odontopterygiform pseudoteeth and lacking the sequential size distribution of the latter, are Anseriformes (large flightless ducks of the tribe Anatini)<sup>36</sup>. Within the hypothesis of a sister-relationship between Anseriformes and Odontopterygiformes<sup>11,29,37</sup>, one could suggest that the

potential of the jaw periosteum to develop bony odontoids might be shared by members of the Odontoanserae, at least. In both moa-nalo and odontopterygiform birds, developmental heterochrony involving jaw growth and rhamphothecal keratinization might be at stake for this potential to be expressed. In the case of moa-nalo, heterochrony related to flightlessness is already assumed for other anatomical parts<sup>38</sup>. A favourable background for the evolution of delayed rhamphothecal keratinization exists in Anseriformes, one of the few bird groups with partly soft rhamphotheca, at least locally, in adults<sup>11</sup>.

### **Supplementary Discussion, section 7. Juvenile specimens provide clues for the growth sequence of the different ranks of pseudoteeth.**

All but two of the odontopterygiform bird specimens with preserved pseudodentition are adults, based on the non-fibrous external aspect of the bone and on the pointed shape of the unbroken pseudoteeth. The two exceptions consist of: (i) a jaw bone fragment of a juvenile of *Lutodontopteryx tethyensis* from the Middle Eocene of Ukraine<sup>30</sup>, and (ii) a jaw bone fragment of a juvenile of cf. *Pelagornis* sp. from the Early Miocene of Venezuela<sup>23</sup> (SFig. 2). Incidentally, the latter fossil was not recognized as a juvenile by the authors, although this is unambiguous. Both fossils exhibit the well-marked fibrous external aspect of the cortical bone, typical of the osteologically juvenile stage. Whereas the adult specimens of *L. tethyensis* from the same locality as the juvenile exhibit three size ranks of pseudoteeth, the juvenile specimen shows only two (PT1s and PT2s). However, tiny caudo-cranially constricted bumps – as constricted as the smallest pseudoteeth of *Pelagornis* – are clearly visible at locations where the third rank pseudoteeth (PT3s) would be expected to develop further toward the adult stage (see fig. 2R in Mayr and Zvonok<sup>30</sup>; reproduced with modifications in SFig. 2). Most of them are emergent PT3s, and show a strongly cranio-caudally constricted elliptical base shape, as in the PT4s of other taxa (except perhaps the first visible bump on the right side, which seems to be a partly broken base, as seen in some PT4 specimens of *P. mauretanicus*<sup>27</sup>). The presence of only two developed size ranks in this juvenile specimen (even though all pseudoteeth are broken due to their fragile, thin cortex), and PT3s only at the bump stage, reflect incomplete development of the pseudodentition at this individual's time of death. This indicates that PT3s start developing later than PT1s and PT2s, in this species at least. Similarly, the juvenile mandible of cf. *Pelagornis* sp. from Venezuela exhibits fully grown PT1s, PT2s, and PT3s (albeit broken), whereas PT4s and probable PT5s are only at the bump stage at the individual's time of death (see fig. 2 in Solórzano and Rincón<sup>23</sup>; reproduced with modifications in SFig. 2). To summarize, PT3s start growing after PT1s and PT2s, and PT4s and PT5s (when present) start growing after the three higher ranks of pseudoteeth. Hence, juvenile odontopterygiform specimens provide evidence for a model of an asynchronous start and a synchronous end of growth for the different ranks of pseudoteeth, with PT1s developing first. Incidentally, the juvenile specimen from Venezuela provides the only evidence that some pseudotoothed birds had five ranks of pseudoteeth (with even additional bumps being irregularly present), albeit with PT4s and PT5s at an early growth stage (SFig. 2). The two juvenile specimens also illustrate the rostro-caudal constriction of smaller pseudoteeth, increasing with rank, which is also obvious in adults of most species. Finally, the ratio between PT1s intervals and jaw bone height is not greater in adult odontopterygiform specimens than in juveniles, which indicates that the relative intervals between PT1s do not increase with growth.

### **Supplementary Discussion, section 8. Interspecific variability in the distribution of pseudoteeth suggests the existence of species-specific characteristics of inhibition zones.**

Differences exist between odontopterygiform species in terms of the distribution and shape of pseudoteeth: height and relative rostro-caudal width of PT1s, spacing between PT1s, ratio

between PT1 measurements and their intervening spaces, width of pseudoteeth divided by width of immediately higher ranked pseudoteeth, or width of pseudoteeth divided by spacing between adjacent pseudoteeth, among other ratios. Among the three-ranked species, a relation exists between the ratio of the interval separating PT1s divided by PT1 width, and the amplitude of the decrease in width of PT3s vs PT2s compared with PT2s vs PT1s (see Supplementary Text 8 table). In species where the value of the distance separating PT1s divided by PT1s width is larger, the decrease in size in a (n) ranked pseudotooth versus a (n-1) ranked pseudotooth is stable from PT1s to PT3s. In contrast, in species where the value of the intervening space between PT1s divided by PT1s width is smaller, the size reduction increases from PT1s to PT3s, and is greater in PT3s vs PT2s, than in PT2s vs PT1s. This suggests that the intervening space between PT1s (coupled with PT1 width) constrains and restricts the size of smaller (lower-ranked) pseudoteeth, including PT3s, which emerge later in our model. This observation conforms to our model of pseudotooth growth control by inhibition from adjacent, higher-ranked (larger) pseudoteeth (we use the pseudotooth base width as the size proxy, rather than height, as pseudotooth tips are generally broken due to post-mortem fractures).

Species	<b>Ratio: PT1 base cranio-caudal width/intervening space between PT1s</b>	PT2 width/PT1 width; PT3 width/PT2 width	<b>Ratio (mean values): (PT3 width/PT2 width) / (PT2 width/PT1 width)</b>
<i>Dasornis emuinus</i> from Morocco	<b>0.18</b>	0.5-0.6; 0.5-0.6	<b>1.00</b>
<i>Dasornis toliapicus</i> from England	<b>0.17</b>	0.7-0.74; 0.6-0.8	<b>0.97</b>
<i>Caspiodontornis kobystanicus</i>	<b>0.17</b>	0.6; 0.5	<b>0.83</b>
<i>Pelagornis chilensis</i>	<b>0.23</b>	0.5-0.6; 0.4-0.5	<b>0.82</b>
<i>Lutetodontopteryx tethyensis</i>	<b>0.25</b>	0.6; 0.4-0.5	<b>0.75</b>
<i>Pelagornis longirostris</i>	<b>0.25</b>	0.5-0.6; 0.3-0.4	<b>0.64</b>

**Supplementary Text 8 table.** The three-ranked odontopterygiform species show a relation between a greater PT1 size vs intervening space (left column in bold), and a greater relative decrease in size from PT2 compared to PT1, toward PT3 compared to PT2 (decreasing ratio between these two ratios, in the right column in bold). Species ordered from no decrease to a greater decrease (right column in bold) are generally ordered from a smaller to a greater ratio (PT1 width/intervening space) (left column in bold). When plotted against each other, the values of these two parameters determine a linear regression with a  $R^2$  of 0.67; the straight line equation is  $y = -2.82x + 1.42$  (in x, ratio: PT1 base cranio-caudal width/intervening space between PT1s; in y, ratio (mean values): (PT3 width/PT2 width)/(PT2 width/PT1 width). NB: four-ranked species values show no difference within these parameters. Data from Supplementary table STable 1.

Other measurements or ratios show no consistent correlations (i) with the presence or absence of PT4s, and (ii) with each other among all species, or among three- to four-ranked species (STable 1). Most species are represented by one or only a few specimens, which might lead to

an overestimation of the interspecific variability in relation to intraspecific variability. Several features still show consistent differences between species, which suggests that species-specific characteristics of inhibition zones and their modifications through development are at stake, such as their strength (radius of action), duration of action, and speed of radius reduction. For instance, the presence of PT4s in certain species (STable 1) might be caused either by a lower radius and/or a faster radius reduction of pseudotooth inhibition zones, or by delayed end of growth (epithelium keratinization).

### **Supplementary Discussion, section 9. Variation in pseudotooth shape in relation to position (rank) adds support to the hypothesis of dynamic inhibition zones.**

Beside the pseudoconical (caniniform) shape of pseudoteeth in all odontopterygiform species, some display other, specific characteristics, such as caudally hooked higher-ranked pseudoteeth (e.g. *P. chilensis*), the presence of a strong basal-apical ridge in caudo-lateral position in higher-ranked pseudoteeth (e.g. *P. mauretanicus*, *P. chilensis*), varying degrees of forward (rostral) slanting in higher-ranked pseudoteeth, or varying degrees of pseudotooth robustness (essentially starting with PT1s; sharp vs obtuse) (STable 1). Beyond these features, pseudoteeth of different ranks also differ in terms of rostro-caudal constriction within all odontopterygiform species<sup>11</sup>. In all species of *Pelagornis* and *Lutetodontopteryx*, PT1s are pseudo-conical, and lower-ranked pseudoteeth are increasingly more constricted rostro-caudally (SFIGS. 3, 4), with PT4s and even PT5s (in species bearing them) being blade-shaped (see SFIG. 2). For instance, in *P. mauretanicus*, the ratios of rostro-caudal width to latero-medial thickness at the base of pseudoteeth range from 1.1 in one PT1, to 0.77 in one PT2, then ~0.65-0.75 in PT3s, and 0.34-0.63 in PT4s<sup>11,27</sup> (SFIG. 3). In species of *Dasornis*, the trend is the same, starting with the base of PT1s being rostro-caudally longer than in *Pelagornis*. In the *Dasornis toliapicus* specimens from the Paleogene of Morocco (SFIG. 4, STable 1), the ratios of rostro-caudal width to latero-medial thickness at the base of the pseudoteeth range from 2.50-4.00 in PT1s (n=3), to 0.92-2.55 in PT2s (n=3), and 0.76-1.15 (n=5) in PT3s. Consequently, in *Dasornis*, the base of pseudoteeth is longer rostro-caudally than the base of pseudoteeth of the same rank in *Pelagornis*, but all species of both genera share a relative increase in rostro-caudal constriction in increasingly smaller (lower-ranked) pseudoteeth.

Incidentally, in *Pelagornis* spp., *L. tethyensis*, and also the *Dasornis emuinus* specimens from Morocco, the latero-medial thickness of tomia equals the latero-medial basal thickness of PT1s, but the smaller pseudoteeth are thinner at their base and located at the lateralmost edge of tomia, so that all pseudoteeth are aligned laterally but not medially (the most “shifted” laterally being the smallest, PT4s or PT3s<sup>11</sup>; SFIG. 3). This suggests that the centres of pseudoteeth development appear at the lateral edge of the tomia. (In the *Dasornis toliapicus* from Morocco, higher-ranked pseudoteeth are relatively thin medio-laterally, so that the tomia are thin as well; therefore, the base of lower-ranked pseudoteeth is barely thinner than the tomia, so that their lateral implantation is not obvious; SFIG. 4).

### **Supplementary Discussion, section 10. Irregular, abnormal distribution of pseudoteeth within some specimens or individuals.**

Irregularities in the presence/absence, exact position, relative size, and/or spacing of pseudoteeth of various ranks occur in almost all of the species/specimens. For instance, in some cases a small, supplementary pseudotooth the size of a PT4 – even in species lacking these – is intercalated between two pseudoteeth but absent from the rest of the jaw (e.g., *P. orri*; see STable 1). Another example is the occurrence of two “small PT2s” side by side, smaller than expected and just slightly larger than the PT3s intervening between them and the much larger PT1s; this is the case in the large ‘*Dasornis*’ specimen from Ukraine described in Mayr and Zvonok (2011: text-fig. 2 A,B)<sup>39</sup>. For some unknown reason, these two PT2s



emerged side by side in place of a single larger expected PT2, and this indeed resulted in their smaller size. In the frame of our model, their smaller size might be explained by the conjunction of a reciprocal inhibition effect from the PT2s themselves, and greater proximity to PT1s, implying longer inhibition. The jaw elements of each species are represented by single individuals (minimum number of individuals based on these jaw elements; MNI= 1; see STable 1), except for *L. tethyensis*, *Dasornis/Gigantornis* from Ukraine, and *D. toliapicus* from Morocco (MNI: near 2 for each), and *P. orri* (MNI: 4 or 5) (STable 1). Even in cases with an MNI above 1, no given part of the jaw can be compared with a homologous part from another individual, due to poor preservation or lack thereof. Therefore, specimens with irregularities stand as isolated cases, and are not easily interpretable in terms of their morphogenetic causes, since several parameters might be involved. For instance, there is the “normal” modification along the jaw (rostro-caudally) in terms of pseudotooth sizes and intervals, in all specimens, and which confounds the “accidental” variations: namely the spacing between pseudoteeth and their size decrease toward the cranial and caudal ends of jaw bones. Incidentally, the latter pattern could be explained by smaller inhibition zones at the jaw’s extremities, because these jaw regions developed later and closer to the end of pseudoteeth growth. Some variations might also be age-related (especially given our hypothesis of the late development of pseudoteeth relative to the rest of the jaw skeleton). Pathology or bone reconstruction following fractures cannot be excluded in some cases. Besides the relative size and spacing of pseudoteeth, irregularities exist also in terms of slant, or even locus of implantation (e.g. in the large *D. emuinus* from Morocco; STable 1).

#### **Supplementary Discussion, section 11. Interpretable irregularities fit with our model of dynamic inhibition zones.**

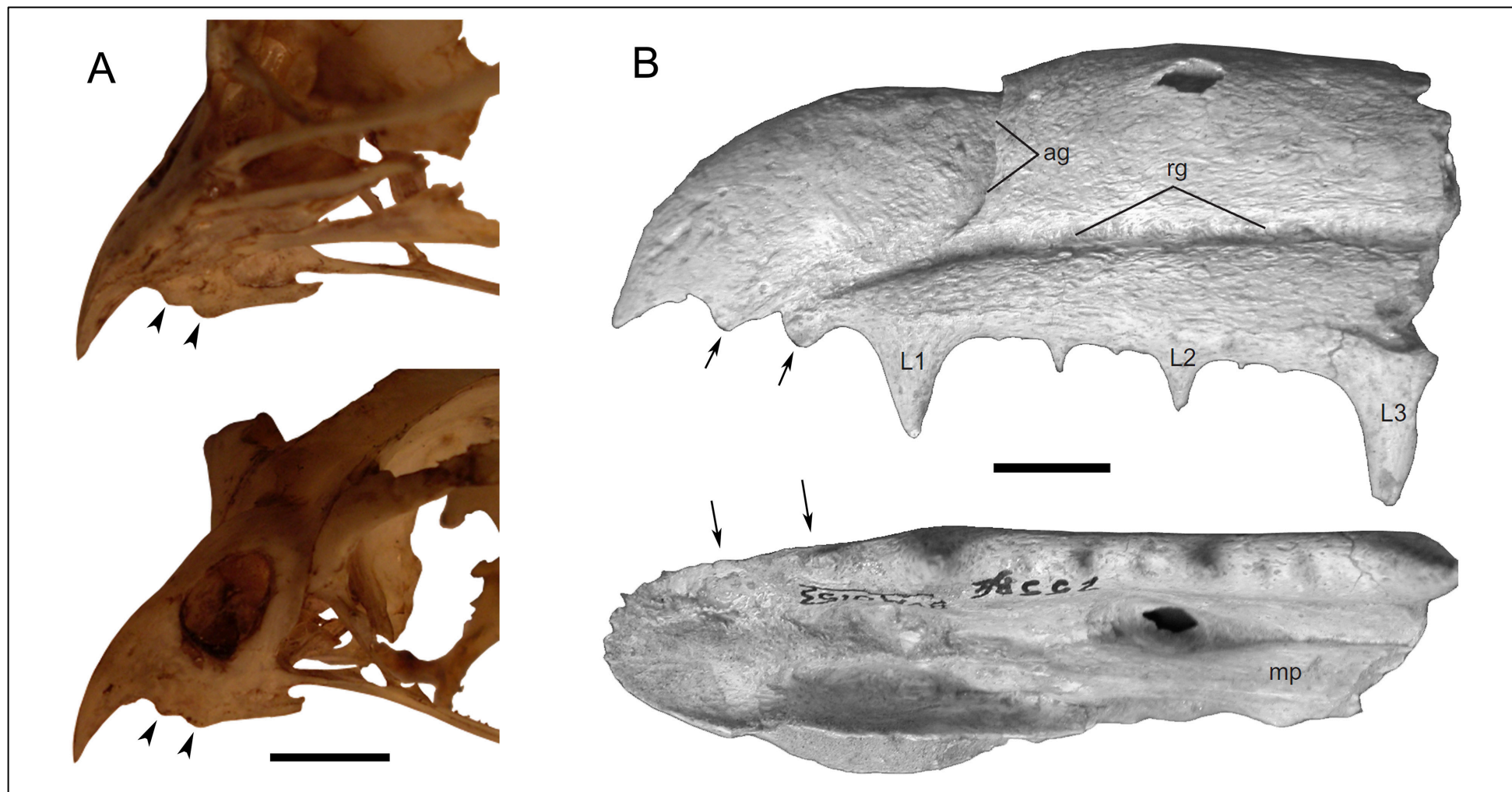
Evaluation of irregularities can be attempted through comparison of a variant with a “control” region, especially when the right and left maxillae are available at the same rostro-caudal level. Such a comparison is possible on a fragment from the premaxillary of a *D. toliapicus* from the Paleogene of Morocco (SFig. 4; STable 1). It reveals that at the same rostro-caudal level there is an interval of 20 mm between two PT1s on the left side, whereas the corresponding interval is only 14.3 mm on the right side. The size (base cranio-caudal width) of intervening PT2s is, respectively, 3.3 mm on the left side (80% of PT1) and 2.1 mm on the right side (50% of PT1). There are no significant differences for PT3s. Hence, a longer spacing between two consecutive PT1s corresponds to a larger intervening PT2. This adds support to our model, in which a longer interval implies a wider (and earlier appearing) inhibition-free zone mid-distance between two pseudoteeth, which makes it possible for the pseudotooth developing at this locus to grow for longer and therefore larger.

#### **Supplementary Discussion, section 12. Evaluating the galloanserine gliding articulation as a factor favouring pseudodentition evolution.**

The “particularities of a galloanserine-like feeding apparatus, such as the gliding jaw joint (e.g. Weber and Hesse 1995)”<sup>40</sup> were suggested as factors favouring the evolution of pseudodentition by Mayr (2011: 458)<sup>29</sup>. The gliding jaw joint is a misleading designation, since the actual feature referred to is a rostro-caudally gliding mandible-quadrangle articulation<sup>41,42</sup>. This gliding articulation is present in advanced pseudotoothed birds (*Pelagornis* spp.)<sup>29</sup>, at least (unknown because anatomical region is not preserved in fossils of more basal pseudotoothed birds). However, besides Galloanserae and *Pelagornis*, this articulation is also present (true homology unknown) in *Hesperornis* and *Ichthyornis*<sup>29</sup>. Therefore, this feature is probably not strictly linked to increased herbivory (*contra* Weber<sup>41</sup>). Furthermore, there are no means by which this characteristic would preferentially favour or allow pseudotooth evolution. Other characteristics were likely involved in the adaptive

function of pseudodontition, namely the streptognathism and the absence of mandibular symphysis<sup>43</sup> (see Main text). Incidentally, these hypotheses concern adaptive factors possibly favouring the evolutionary emergence and persistence of pseudodontition, and do not pertain to their ontogenetic determinants. As such, these two types of causes, distal and proximal, should not be confused.

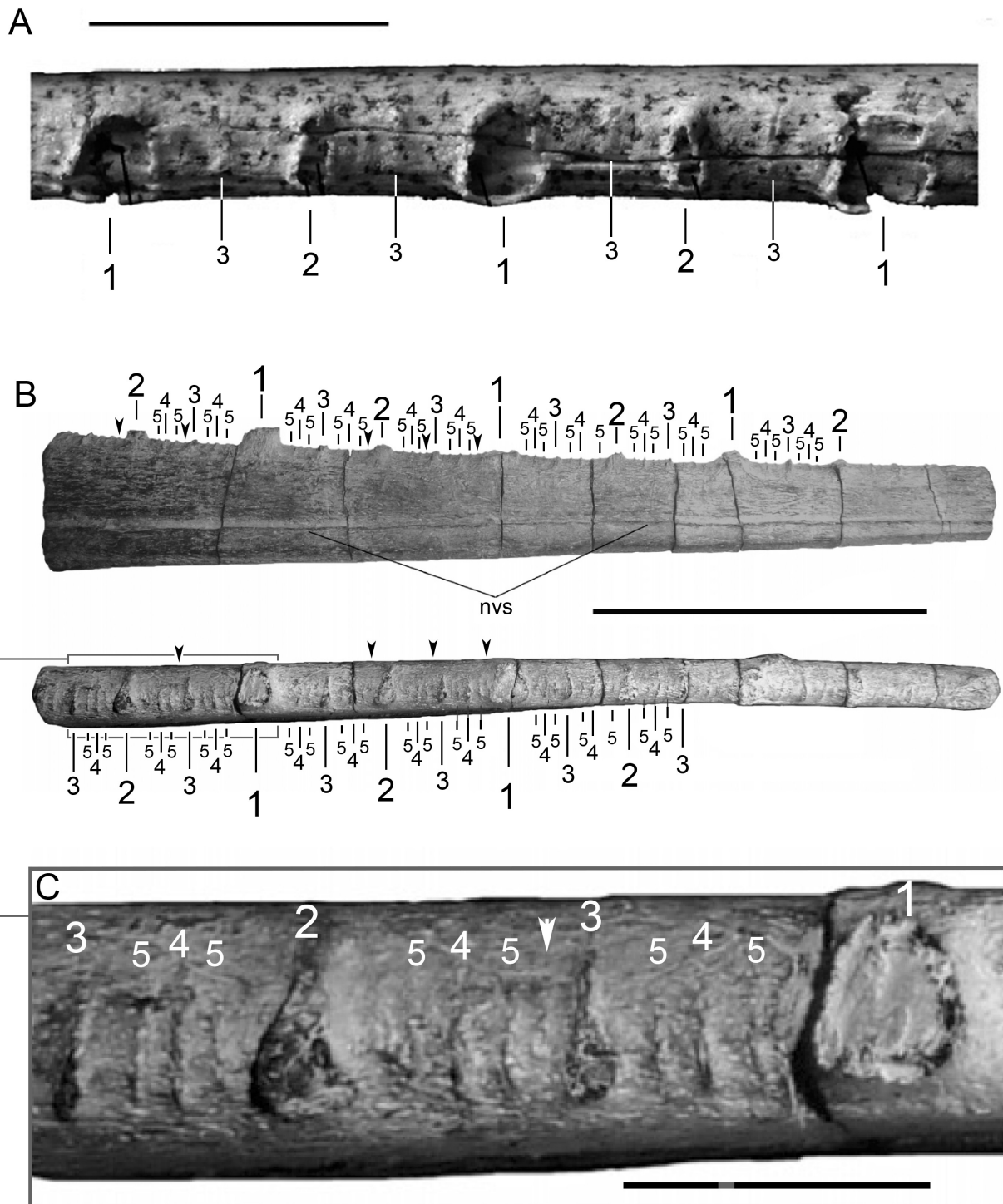
## Supplementary Figures



**Supplementary Figure 1.** “Tomial teeth” in an extant bird and a pseudotoothed bird.

**A**, bony rostrum of extant *Harpagus bidentatus* (Aves, Accipitridae), rostral part. Natural light photographs. Top: medio-ventral view of the right pair of “tomial teeth”; bottom: lateral view of the left pair. Arrows indicate the paired “tomial teeth” of *H. bidentatus* that are double, rounded, lateromedially constricted, and located at the rostral tip of the rostrum. These are only bony extensions of the blade-like tomia, and are paralleled by the external shape of the rhamphotheca. **B**, bony rostrum of the extinct *Pelagornis (Osteodontornis) orri* (Aves, Odontopterygiformes), rostral part. Modified from ([22]: fig. 2; *Paleobios*, journal of the Museum of Vertebrate Zoology, University of California Berkeley, USA). Top: left lateral view; bottom: ventral view. These odontopterygiform “tomial teeth” are similar to those of *H. bidentatus*, and other odontopterygiforms (SText 3).

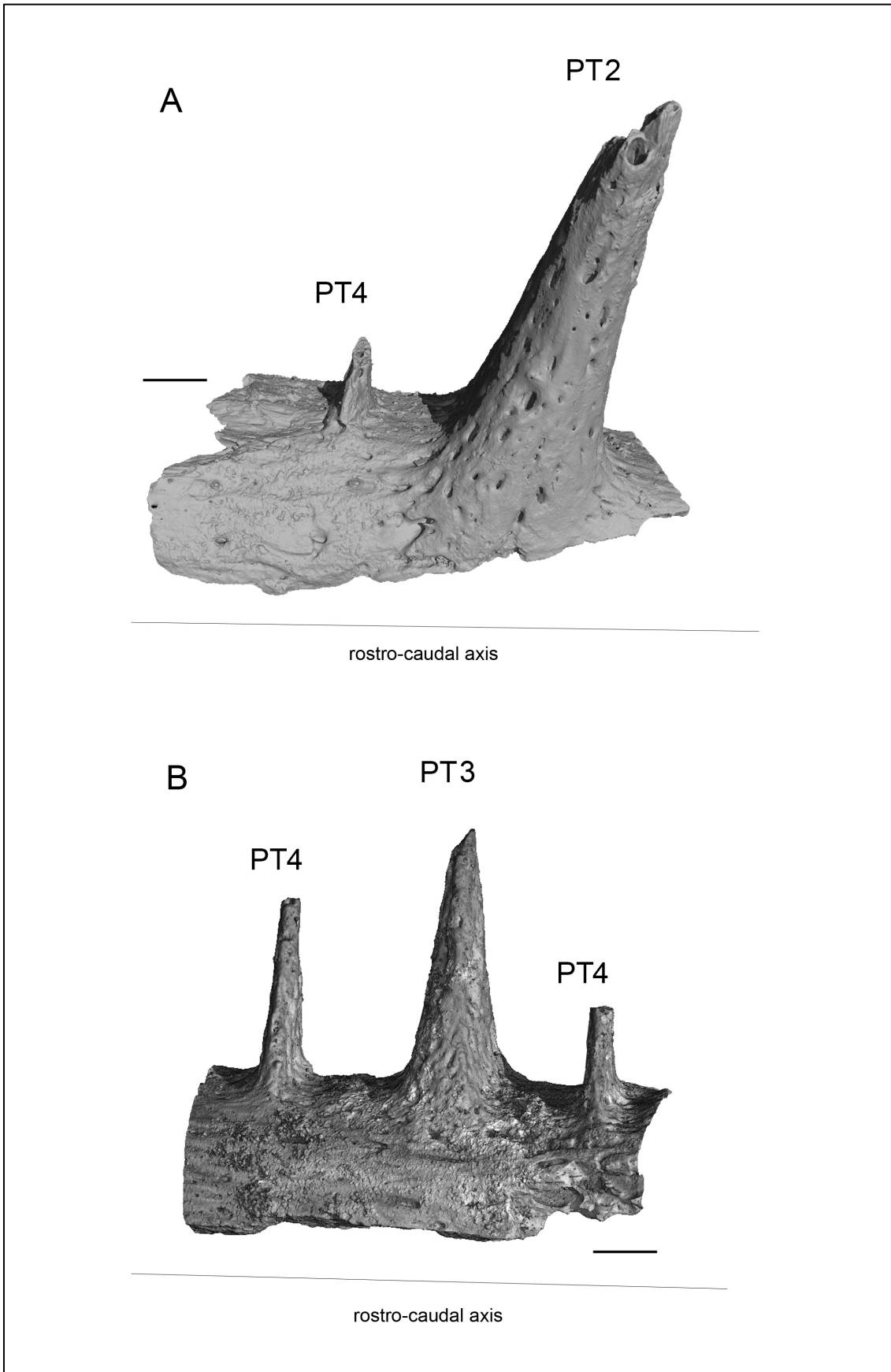
They possibly grew synchronously with the main jaw bone, as opposed to pseudoteeth which grew after the end of the main jaw growth (see SText 3). ag, anterior groove; mp, medial palatal ridge; rg, rostral groove; L1-3, large pseudoteeth 1-3 (all nomenclature after Stidham<sup>22</sup>). Scale bars, 10 mm.



**Supplementary Figure 2.** Juvenile pseudodontitions reveal growth sequence of pseudoteeth.

**A**, Rostral part of right mandibular ramus of juvenile pseudotoothed bird *Lutetodontopteryx tethyensis* from the Middle Eocene of Ukraine, modified from ([30]: fig. 2R; *Journal of Vertebrate Paleontology*, Taylor & Francis Ltd., <http://www.informaworld.com>). Dorsal view showing broken pseudoteeth 1 and 2 (fully, or almost, grown, owing to their width), and PT3s at bump stage (only starting growth). The latter later developed into PT3s visible between PT1s and PT2s in adults of the same species. **B**, right mandibular ramus in a juvenile of

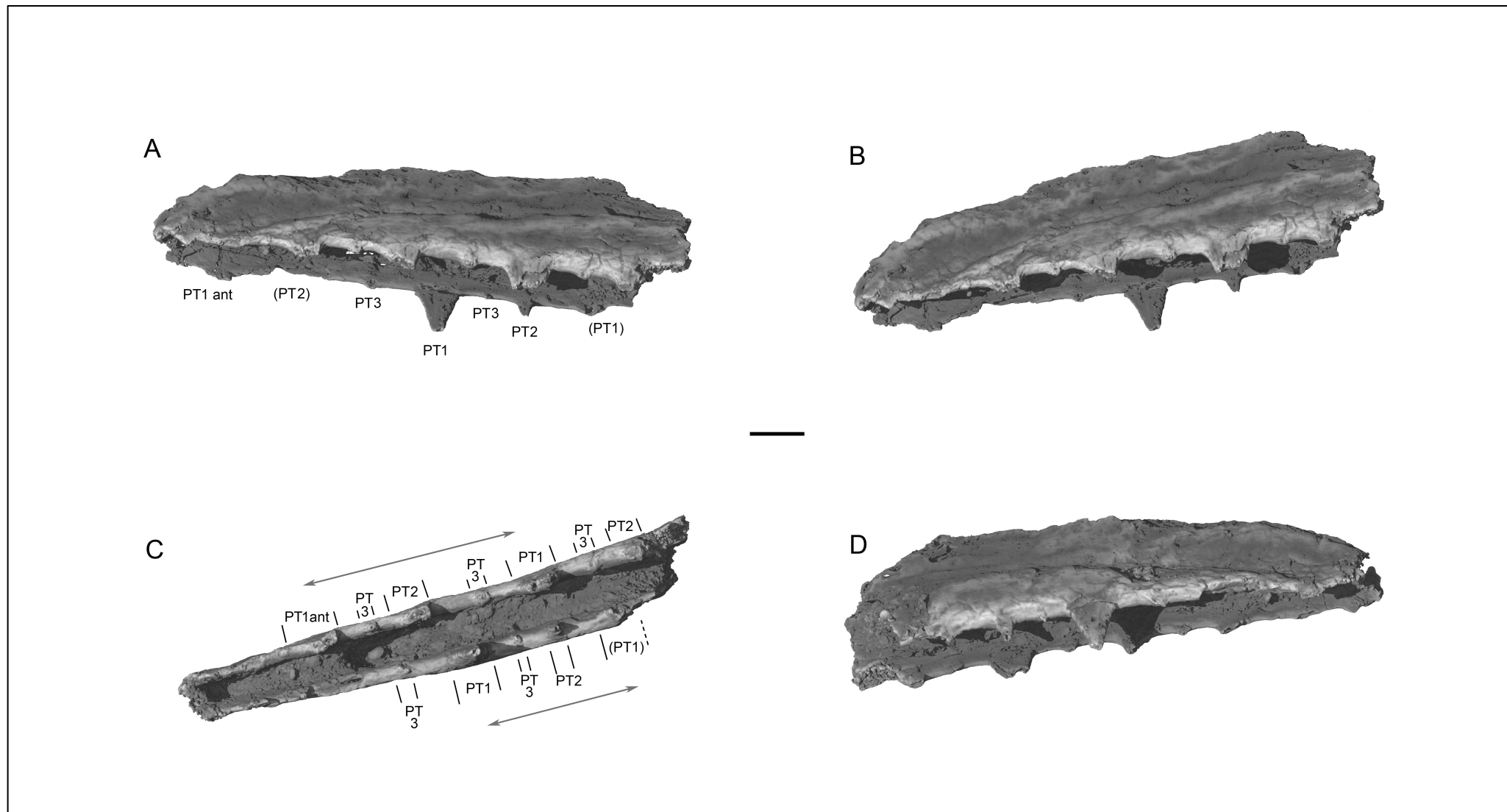
cf. *Pelagornis* sp., from the Early Miocene of Venezuela, modified from ([23]: fig. 2B,C; *Journal of Vertebrate Paleontology*, Taylor & Francis Ltd., <http://www.informaworld.com>); lateral (top) and occlusal view (bottom). The rank of pseudoteeth is indicated by numbers 1 to 5. Insert **C**, magnification of the area indicated in (**B**), illustrating the difference between pseudoteeth broken at their base, and bumps (pseudoteeth at an early growth stage), modified from ([23]: fig. 2C). In **A**, **B** and **C**, figure parts from [23] and [30] reprinted, with modification, by permission of the Society of Vertebrate Paleontology, [www.vertpaleo.org](http://www.vertpaleo.org). This figure is not covered by the CC BY licence. Credits to copyright-holder, Taylor & Francis Ltd. for panels S2A, S2B and S2C. All rights reserved, used with permission. In (**B**) and (**C**), five ranks occur (fourth and fifth at bump stage), a case unique in pseudotoothed birds. In addition, intervening bumps can even be identified irregularly (arrowheads). In (**B**) and (**C**) the pseudodentition is at a comparatively more advanced growth stage than in (**A**), since broken PT3s are fully grown (almost like PT1s and PT2s), and not simple bumps; in (**B**) and (**C**) PT4s and PT5s are at the bump stage, and in (**A**) the PT3s are at bump stage. The juvenile status of both fossils is obvious because of the fibrous aspect of the bone surface. These fossils clearly indicate that lower-ranked (smaller) pseudoteeth start growing later than higher-ranked (larger) ones (SText 7). The two fossils also illustrate the rostro-caudal constriction of pseudoteeth, visible since the earliest growth stages, and increasing with rank. Scale bars, 10 mm (**A**), 50 mm (**B**), 10 mm (insert **C**).



**Supplementary Figure 3.** Pseudoteeth of *Pelagornis mauretanicus* as seen in X-ray microtomographic views. **A**, specimen AaO-PT-B in medial-apical view, and **B**, specimen AaO-PT-A in lateral view<sup>11</sup>. Increasingly lower-rank (smaller) pseudoteeth are increasingly constricted rostro-caudally (the most constricted are the PT4s) (see S.Text 9). The numbers indicate the rank of each pseudotooth. In all the pseudoteeth, the apex is

broken to varying degrees, due to post-mortem breakage; in **(B)** the right PT4 lacks more of the apex than the left PT4. Scale bars, 2 mm.





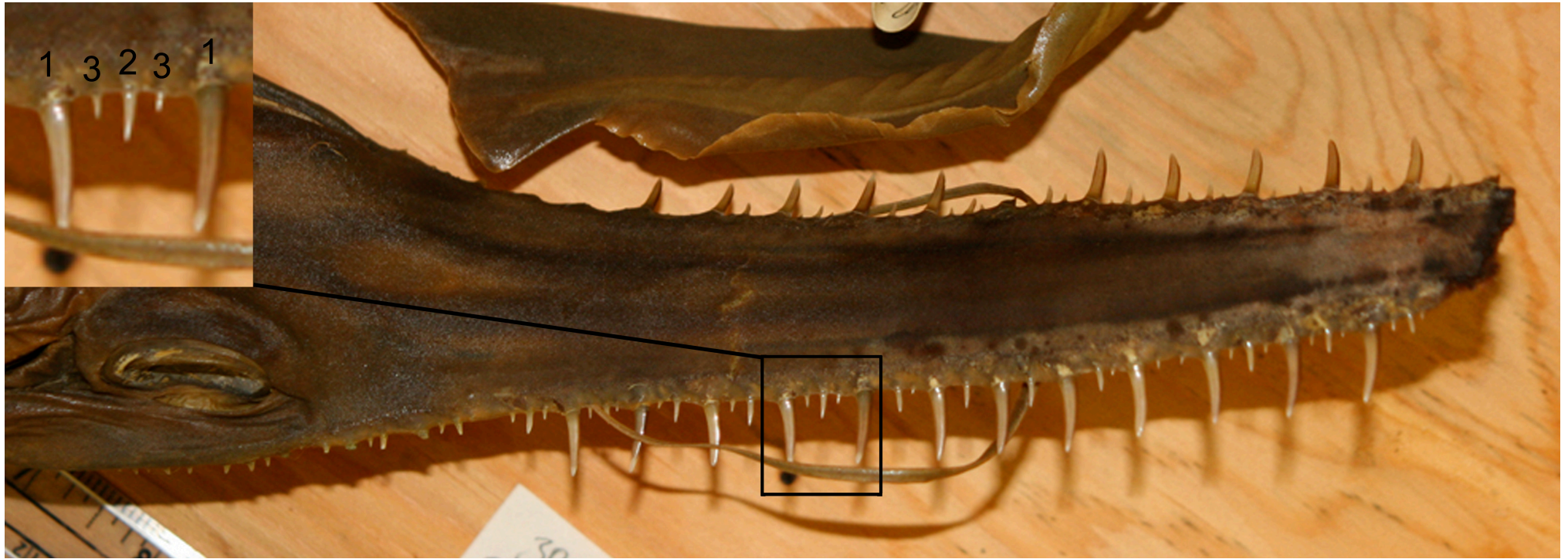
**Supplementary Figure 4.** Rostrum of *Dasornis toliapicus* from the Paleogene of Morocco as seen in X-ray microtomographic views. Distribution and shape of the pseudoteeth of various ranks, on left vs right sides. **A**, **B**, left latero-ventral views; **C**, ventral view; **D**, right latero-ventral view. Increasingly lower-ranked (smaller) pseudoteeth are increasingly constricted rostro-caudally (see SText 9). Spacing between PT1s (grey lines with arrows in **C**) is wider on the left side than on the right, and the intervening PT2 is larger on the left side, which adds support to our dynamic inhibition zone model (see SText 11). Scale bar, 5 mm.



**Supplementary Figure 5.** Dentition of *Cynodon gibbus* (Agassiz, 1829) (Order Characiformes, Family Cynodontidae).

Copyright Adam Carvalho. Modified from: <https://www.flickr.com/photos/sickilla/5169310782/>

Natural light photograph. Insert shows size classes of true teeth (numbers), arranged exactly as in a pseudodentition. The size distribution of teeth parallels that of pseudoteeth in the odontopterygiform species, in this case with up to four size ranks, though two “rank 4” teeth are lacking in the example (locations indicated by asterisks).



**Supplementary Figure 6.** Dentition of the “saw” (rostrum) of the saw-shark *Pristiophorus cirratus* (Latham, 1794) (Order Pristiophoriformes, Family Pristiophoridae). Copyright Museum of Comparative Zoology, Harvard University, USA. Modified from: [http://mczbase.mcz.harvard.edu/specimen\\_images/fish/large/38611\\_Pristiophorus\\_cirratus\\_rostrum.jpg](http://mczbase.mcz.harvard.edu/specimen_images/fish/large/38611_Pristiophorus_cirratus_rostrum.jpg)  
Source URL: <https://mczbase.mcz.harvard.edu/guid/MCZ:lch:38611> ; taxonomic search on <https://mczbase.mcz.harvard.edu/>  
Natural light photograph. Insert shows size classes of true teeth (numbers) that are arranged exactly as in a pseudodentition. In this example, the dentition parallels a three-ranked pseudodentition.

Supplementary Table

Species (/specimen)	PT1 cranio-caudal width at base (not too cranial or caudal PT1s)	PT1 height (not too width at cranial or caudal PT1s)	PT1 cranio-caudal base/height ratio (robustness)	interval between PT1s	beak length	length from PT1 base cranio-caudal width/length X 100 (%)	length from naso-frontal hinge to caudal end of skull	(PT1 base cranio-caudal width/length from naso-frontal hinge to caudal end of skull) X 100 (%)	PT1 base cranio-caudal width/intervening space between PT1s	PT1 height/intervening space between PT1s	PT2 base cranio-caudal width/PT1 base cranio-caudal width	PT2 base cranio-caudal width/interval between surrounding PTs	PT3 base cranio-caudal width/PT2 base cranio-caudal width	PT4 base cranio-caudal width/PT3 base cranio-caudal width	partly discriminant PT shape attributes	slant of PTs (or absence)	normal distribution of PT ranks	irregularities	geological age	number of specimens (MN) with jaw parts	references
<i>Pelagornis mauretanicus</i>	8.0-9.0	16.0-20.0	0.45-0.5	37.0-42.0 (mean 39.8; n=4)	-	-	-	-	0.21	0.45	0.6-0.7; 0.5; 0.3-0.4	0.224-0.245; 0.106-0.14; 0.09-0.12	-	-	PTs slender, conical, not recurved; PTs 1 and (2) with caudo-lateral ridge	PT4s vertical, but larger PTs progressively slant forward: mandible PTs ca. 6° to 15°; rostrum PTs ca. 5° (rostral end PTs)	1-4-3-4-2-4-3-4-1	minimal: only in height of some PTs, late Pliocene-early but not in their presence/position	Pleistocene limit	1	11,27
<i>Pelagornis stirtoni</i>	5.7	14.3	0.4	ca 25.0	-	-	-	-	0.23	0.57	ca. 0.4; 70.5	-	-	PTs slender, slightly recurved; PT3s described as spines; no caudo-lateral ridge visible	slant forward: ca 15° (mandible PTs, rostral end)	1-3-2-3-1		Miocene/Pliocene	1	44	
<i>Pelagornis chilensis</i>	12.5-15.6	21.9-25.5e	0.49-0.65	53.9-76.0 (mean 61.5; n=5)	361.0	4.0-4.4	144.0	10.1-11.0	0.23	0.39	0.5-0.6; 0.4-0.5	0.12-0.16; 0.12-0.15	-	-	PTs robust, recurved caudally (but variably: only the cranialmost ones; mandible: cranial ones and less so the caudal ones); caudo-lateral ridge (rostrum PT1s, mandible: PT1s and PT2s)	varied slant: mandible PTs 0° (rostral end) to ca. 15° forward (caudal end); rostrum PTs: ca -18° (ie backwards; rostral end) to 0° (middle) to ca +18° (ie forward; caudal end)	1-3-2-3-1	intercalation of a small supplementary PT (equivalent to a PT4) at least at 5 locations of rostrum between PT1s and PT3s (Mayr and Rubilar 2010; fig. 18)	middle Miocene-earliest Pliocene	1	19
<i>Pelagornis orri</i>	7.0-12.0	13.0-19.5e	0.52-0.62	30.0-40.0 (mean 35; n=4)	300.0	2.9-3.3	100.0	8.8-10.0	0.27	0.46	0.5-0.6; 0.5-0.7; ca. 0.4	0.11 (n=2); 0.11-0.17; 0.07-0.13	-	-	PTs robust, only the cranialmost ones being slightly recurved caudally; no visible caudo-lateral ridge	slight slant forward at caudal part of mandible (ca +10°); slight slant backward for PTs at rostral part of rostrum (ca -5° -8° to -18°); other parts: 0°	1-4-3-4-2-4-3-4-1 1-3-2-3-1; it is clear that traces of PT3s bases are visible, especially on mandible, probably eroded due to poor preservation, and despite assertions to the contrary (Howard 1957, Howard and White 1962, among others)	few: only in height of some PTs, but less in their presence/position; eg a PT4 larger than a PT3 and almost as large as a PT2 - and variation in intervals too, within a single specimen (rostrum in Olson 1985; fig. 9; similar example in mandible in Stidham 2004; fig. 4); isolated change in slant in a PT3 in Howard and White (1962; figure 3) - ca -20° vs. 0°	middle and late Miocene	4 or 5	22,32,33,45,46
<i>Pelagornis longirostris</i>	13.3-15.9	ca 21.0e-25.0e	0.57-0.64	55.5-63.5 (mean 58.3; n=4)	-	-	ca. 200.0	6.7-8.0	0.25	0.39	0.5-0.6; 0.3-0.4	0.15; -	-	-	PTs robust, not recurved	slant forward: mandible PTs ca 4°-11°; rostrum PTs no slant visible (but poor preservation)	1-4-3-4-2-4-3-4-1 1-3-2-3-1; PT4s present irregularly but which is a feature of the species and not an artifact of preservation	?	1	47,48	
<i>Pelagornis sandersi</i>	11.3; 8.87; 6.86	16.1; 16.9; 13.3; 11.3	0.61; 0.67; 0.67; 0.7	46.0; 56.5	405.0	2.2; 1.7; 2.79	161.0	5.5; 4.3; 7.0	0.19; 0.15; 0.20	0.30	0.53-0.55; 0.52-0.65	0.105-0.106; 0.11-0.13	-	-	PTs not recurved; caudo-lateral ridge on larger rank PTs	slant forward of mandible PTs: ca 8° to 15° (rather rostral part of mandible)	1-4-3-4-2-4-3-4-1	important irregularities	late Oligocene	1	24,43
<i>Pelagornis sp. Japan Miocene</i>	8.8	-	-	42.4	-	-	-	-	0.21	-	0.63; 0.5; 0.4	0.14; 0.13-0.14; 0.09-0.1	-	-	PTs slightly recurved; apparently no caudo-lateral ridge	when clearly assessable: no slant visible	1-3-2-3-1	alleged great irregularity is in fact due to poor preservation	late Early Miocene (17.5-17 Ma)	1	49
<i>Caspiodornis kobaystonicus</i>	8.4-8.8	16.7-	0.5	51.0	ca. 227.0	3.7-3.9	ca. 93.0	9.0-9.5	0.17	0.33	0.6; 0.5	0.11-0.12; 0.09-0.1	-	-	PTs not recurved		1-3-2-3-1		Oligocene	1	50
<i>Lutetodontopteryx lethynensis</i>	4.2-4.6	9.3-10.0	0.45-0.46	17.3-17.9 (mean 17.7; n=3)	-	-	-	-	0.25	0.55	0.6; 0.4-0.5	0.16-0.18; 0.16-0.18	-	-	PTs slender, not recurved caudally; caudo-lateral ridge absent or faint	slant forward (mandible PTs): 17°	1-3-2-3-1		middle Eocene	2 (1 ad., 1 juv.)	30,39
<i>Dasornis sp. / ?Gigantornis sp. Ukraine</i>	8.5-10.0	12.5-15.9	0.63-0.68	53.7	-	-	-	-	0.17	0.26	0.4; 0.6	-	-	PTs robust, not recurved; apparently no caudo-lateral ridge	larger PTs of middle mandible: slant forward ca 10°	1-3-2-3-1		middle Eocene	2	30,39	
<i>Dasornis emilinus</i> Morocco (NB: a wide sulcus medially and ventrally on mandible is unlike other pseudotoothed birds except the <i>Dasornis</i> ?/ <i>Gigantornis</i> of Ukraine (and absence of sternum known for Moroccan fossils allow possibility of <i>Gigantornis</i> ))	7.0-9.0	-	-	39.5; 47.5	-	-	-	-	0.18	-	0.5-0.6; 0.5-0.6	-	-	Caudo-lateral ridge present	apparently (PTs broken off) none	1-3-2-3-1	two mandibular PTs project dorso-laterally rather than dorsally, in a faint apical tomial groove, from where all PTs emerge, but which locally deviates laterally.	late Paleocene-early Eocene	1	51; present study	
<i>Dasornis tollapica</i> England	2.5	5.5	0.45	15.0	-	-	-	-	0.17	0.37	0.7-0.74; 0.6-0.8	0.11; 0.12, 0.13; 0.17.	-	-	strong slant forward (caudal part of rostrum and mandible - the only jaw parts known): ca 27°	1-3-2-3-1		early Eocene	1	51,52	
<i>Dasornis tollapicus</i> Morocco	4.0-4.3	6.0e	0.67	14.8 (right side); 20.0 (left side) (mean 17.4; n=2)	-	-	-	-	ca. 0.30 (large interval: interval: left side); 0.21 (large interval: interval: left side); 0.28 (small interval: interval: right side); see Text and Supplementary Text	ca. 0.41 (small interval: interval: right side); large interval (20, left): 0.8; 0.4-0.5; small interval (14.8, right): 0.5; 0.5	0.19; 0.11-0.2	-	-	PTs robust, not recurved; caudo-lateral ridge seen on one PT only (PT1).	no slant (at least at rostral part of rostrum and mandible, and caudal part of rostrum, ie differs from English <i>D. tollapica</i> )	1-3-2-3-1	there is a strong asymmetry between left and right side of rostrum: it is not only a shift of PT positions left vs right, but also different spacings of PTs between the two sides (locally larger intervals on left side).	late Paleocene-early Eocene	2 or 3	51; present study	

**Supplementary Table 1.** Measurements and observations on the pseudodontation in species (or specimens) of pseudotoothed birds for which jaw material is available.

These data do not include parts of jaws in which irregularities or abnormalities occur (except when useful and presented as irregularities *per se*). Also, these data do not concern the rostral and caudal ends of jaws, in which pseudotooth size and spacing decrease compared to those of identical rank pseudoteeth located in the middle part of a row. Measurements are in millimetres, and taken only where the fossil part is not broken. e, estimated measurement; -, no data available / no measurement possible. Pseudotooth height is measured from the tomium adjacent to pseudotooth base, and orthogonal to the tomium. The intervening space (interval) between two pseudoteeth is measured along the tomium between the mid-points of each pseudotooth basal plate. Pseudotooth width is measured rostro-caudally (which would correspond to "length" in true tooth measurement methodology). Only adult specimens are included.

## Supplementary References

1. Stettenheim, P. R. The integumentary morphology of modern birds – an overview. *Amer. Zool.* **40**, 461–477 (2000).
2. Rand, A. L. On the spurs of birds' wings. *Wilson Bull.* **66**, 127–134 (1954).
3. Beauchamp, A. J. The ageing of Weka (*Gallirallus australis*) using measurements, soft parts, plumage and wing spurs. *Notornis* **45**, 167–176 (1998).
4. Juhn, M. Spur growth and differentiation in the adult thiouracil-treated fowl. *Physiol. Zool.* **25**, 150–162 (1952).
5. Juhn, M. Functional persistence of embryonic determinations in feathers and late developmental stages in spurs. *Ann. New York Acad. Sci.* **55**, 133–141 (1952).
6. Puchkov, V. F. The development of spur germs in chick embryo. *Arkhiv Anatomii, Gistologii i Embriologii* [in Russian] **76**, 32–41 (1979).
7. Davison, G. W. H. Avian spurs. *J. Zool.* **206**, 353–366 (1985).
8. Howard, H. Observations on young tarsometatarsi of the fossil turkey *Parapavo californicus* (Miller). *Auk* **62**, 596–603 (1945).
9. Peters, J. Zum Stand der Hühnerhaltung in der Antike. *Beitr. z. Archäozool. u. Prähist. Anthropol.* **1**, 42–58 (1997).
10. Sadler, P. The use of tarsometatarsi in sexing and ageing domestic fowl (*Gallus gallus* L.), and recognising five toed breeds in archaeological material. *Circaea* **8**, 41–48 (1991).
11. Louchart, A. *et al.* Structure and growth pattern of pseudoteeth in *Pelagornis mauretanicus* (Aves, Odontopterygiformes, Pelagornithidae). *PLoS ONE* **8**, e80372 (2013).
12. Olson, S. L. & James, H. F. Descriptions of thirty-two new species of birds from the Hawaiian Islands: part I. Non-passeriformes. *Ornithol. Monogr.* **45**, 1–88 (1991).
13. Fabrezi, M. & Emerson, S. B. Parallelism and convergence in anuran fangs. *J. Zool. Lond.* **260**, 41–51 (2003).
14. Currey, J. D. Mechanical properties and adaptations of some less familiar bony tissues. *J. Mech. Behav. Biomed.* **3**, 357–372 (2010).
15. Britz, R., Conway, K. W. & Rüber, L. Spectacular morphological novelty in a miniature cyprinid fish, *Danionella dracula* n. sp. *Proc. R. Soc. B* **276**, 2179–2186 (2009).
16. Gaffney, E. S. Comparative cranial morphology of recent and fossil turtles. *Bull. Amer. Mus. Nat. Hist.* **164**, 65–376 (1979).
17. Martill, D. M. A functional odontoid in the dentary of the Early Cretaceous pterosaur *Istiodactylus latidens*: Implications for feeding. *Cret. Res.* **47**, 56–65 (2014).
18. Harrison, C. J. O. & Walker, C. A. A review of the bony toothed birds (Odontopterygiformes): with descriptions of some new species. *Tert. Res. Spec. Paper* **2**, 1–62 (1976).
19. Mayr, G. & Rubilar-Rogers, D. Osteology of a new giant bony-toothed bird from the Miocene of Chile, with a revision of the taxonomy of Neogene Pelagornithidae. *J. Vertebr. Paleont.* **30**, 1313–1330 (2010).
20. Seki, Y. *Structure and mechanical behavior of bird beaks*. PhD Dissertation, University of California, San Diego (2009). Permalink: <http://escholarship.org/uc/item/7064f0k0>
21. Louchart, A. & Viriot, L. From snout to beak: the loss of teeth in birds. *Trends Ecol. Evol.* **26**, 663–673 (2011).
22. Stidham, T. A. New skull material of *Osteodontornis orri* (Aves: Pelagornithidae) from the Miocene of California. *PaleoBios* **24**, 7–12 (2004).
23. Solórzano, A. & Rincón, A. D. The earliest record (early Miocene) of a bony-toothed bird from South America and a reexamination of Venezuelan pelagornithids. *J. Vertebr. Paleont.* **35**: e995188 (2015).

24. Ksepka, D. T. Flight performance of the largest volant bird. *Proc. Natl Acad. Sci. USA* **111**, 10624–10629 (2014).
25. Reid, K., Prince, P. A. & Croxall, J. P. Fly or die: the role of fat stores in the growth and development of Grey-headed Albatross *Diomedea chrysostoma* chicks. *Ibis* **142**, 188–198 (2000).
26. Granadeiro, J. P. The breeding biology of Cory's Shearwater *Calonectris diomedea borealis* on Berlenga Island, Portugal. *Seabird* **13**, 30–39 (1991).
27. Mourer-Chauviré, C. & Geraads, D. The Struthionidae and Pelagornithidae (Aves: Struthioniformes, Odontopterygiformes) from the late Pliocene of Ahl Al Oughlam, Morocco. *Oryctos* **7**, 169–194 (2008).
28. Harris, M. P., Hasso, S. M., Ferguson, M. W. J. & Fallon, J. F. The development of archosaurian first-generation teeth in a chicken mutant. *Curr. Biol.* **16**, 371–377 (2006).
29. Mayr, G. Cenozoic mystery birds – on the phylogenetic affinities of bony-toothed birds (Pelagornithidae). *Zool. Scr.* **40**, 448–467 (2011).
30. Mayr, G. & Zvonok, E. A new genus and species of Pelagornithidae with well-preserved pseudodentition and further avian remains from the middle Eocene of the Ukraine. *J. Vertebr. Paleont.* **32**, 914–925 (2012).
31. Dumont, M. *et al.* Synchrotron imaging of dentition provides insights into the biology of *Hesperornis* and *Ichthyornis*, the "last" toothed birds. *BMC Evol. Biol.* **16**, 178 (2016).
32. Howard, H. A gigantic "toothed" marine bird from the Miocene of California. *Bull. Dept. Geol. Santa Barbara Mus. Nat. Hist.* **1**, 1–23 (1957).
33. Howard, H. & White, J. A. A second record of *Osteodontornis*, Miocene "toothed" bird. *Los Angeles Cnty Mus. Contrib. Sci.* **52**, 1–12 (1962).
34. Westergaard, B. & Ferguson, M. W. J. Development of the dentition in *Alligator mississippiensis*: upper jaw dental and craniofacial development in embryos, hatchlings, and young juveniles, with a comparison to lower jaw development. *Am. J. Anat.* **187**, 393–421 (1990).
35. Sire, J. Y., Davit-Béal, T., Delgado, S., van der Heyden, C. & Huysseune, A. First-generation teeth in non-mammalian lineages: evidence for a conserved ancestral character? *Microscop. Res. Techn.* **59**, 408–434 (2002).
36. Sorenson, M. D. *et al.* Relationships of the extinct moa-nalos, flightless Hawaiian waterfowl, based on ancient DNA. *Proc. R. Soc. Lond. B* **266**, 2187–2193 (1999).
37. Bourdon, E. Osteological evidence for sister group relationship between pseudo-toothed birds (Aves: Odontopterygiformes) and waterfowls (Anseriformes). *Naturwissenschaften* **92**, 586–591 (2005).
38. Iwaniuk, A. N., Nelson, J. E., James, H. F. & Olson, S. L. A comparative test of the correlated evolution of flightlessness and relative brain size in birds. *J. Zool. Lond.* **263**, 317–327 (2004).
39. Mayr, G. & Zvonok, E. Middle Eocene Pelagornithidae and Gaviiformes (Aves) from the Ukrainian Paratethys. *Palaeontology* **54**, 1347–1359 (2011).
40. Weber, E. & Hesse, A. The systematic position of *Aptornis*, a flightless bird from New Zealand. *Cour. Forsch.-Inst. Senckenberg* **181**, 293–301 (1995).
41. Weber, V. E. Zur Evolution basicranialer Gelenke bei Vögeln, insbesondere bei Hühner- und Entenvögeln (Galloanseres [sic]). *Z. zool. Syst. Evolut-forsch.* **31**, 300–317 (1993).
42. Ericson, P. G. P. The skeletal evidence for a sister-group relationship of anseriform and galliform birds – a critical evaluation. *J. Avian Biol.* **27**, 195–202 (1996).
43. Zusi, R. L. & Warheit, K. I. On the evolution of intraramal mandibular joints in pseudodontorns (Aves: Odontopterygia). *Nat. Hist. Mus. Los Angeles Cnty Sci. Ser.* **36**, 351–360 (1992).

44. Howard, H. & Warter, S. L. A new species of bony-toothed bird (Family Pseudodontornithidae) from the Tertiary of New Zealand. *Rec. Canterbury Mus.* **8**, 345–357 (1969).
45. Howard, H. Additional avian records from the Miocene of Kern County, California with the description of a new species of fulmar (Aves: Procellariidae). *Bull. South. Cal. Acad. Sci.* **83**, 84–89 (1984).
46. Olson, S. L. in *Avian Biology* (eds D. S. Farner, J. R. King & K. C. Parkes) 79–252 (Academic Press, 1985).
47. Spulski, B. *Odontopteryx longirostris* n. sp. *Zeitschrift der deutschen geologischen Gesellschaft* **62**, 507–521 (1910).
48. Lambrecht, K. Studien über fossile Riesenvögel. *Geologica Hungarica, Series Palaeontologica* **7**, 1–37 (1930).
49. Matsuoka, H., Sakakura, F. & Ohe, F. A Miocene pseudodontorn (Pelecaniformes: Pelagornithidae) from the Ichishi Group of Misato, Mie Prefecture, Central Japan. *Paleont. Res.* **2**, 246–252 (1998).
50. Aslanova, S. M. & Burchak-Abramovich, N. I. [An Oligocene pseudodontornithid bird from Perekiškjul' village (Apšeronskij Peninsula)—the first and only record from the USSR and the Asian continent]. *Izvestija Akademii Nauk Gruzinskoj SSR, Seriya Biologičeskayaa* **8**, 406–412 (1982). [Russian]
51. Bourdon, E., Amaghzaz, M. & Bouya, B. Pseudotoothed birds (Aves, Odontopterygiformes) from the early Tertiary of Morocco. *Am. Mus. Novit.* **3704**, 1–71 (2010).
52. Owen, R. Description of the skull of a dentigerous bird (*Odontopteryx toliapicus* [sic], Ow.) from the London Clay of Sheppey. *Quart. J. Geol. Soc. London* **29**, 511–521 (1873).